Elyahb Allie Kwizera
Fischell Department of Bioengineering,
University of Maryland,
8278 Paint Branch Drive,
College Park, MD 20742
e-mail: akwizera@umd.edu

Samantha Stewart
Fischell Department of Bioengineering,
University of Maryland,
8278 Paint Branch Drive,
College Park, MD 20742
e-mail: sstew@umd.edu

Md Musavvir Mahmud
Fischell Department of Bioengineering,
University of Maryland,
8278 Paint Branch Drive,
College Park, MD 20742
e-mail: mmahmud1@umd.edu

Xiaoming He[1]
Fischell Department of Bioengineering,
University of Maryland,
8278 Paint Branch Drive,
College Park, MD 20742;
Marlene and Stewart Greenebaum
Comprehensive Cancer Center,
University of Maryland,
Baltimore, MD 21201
e-mail: shawnhe@umd.edu

Magnetic Nanoparticle-Mediated Heating for Biomedical Applications

Magnetic nanoparticles, especially superparamagnetic iron oxide nanoparticles (SPIONs), have attracted tremendous attention for various biomedical applications. Facile synthesis and functionalization together with easy control of the size and shape of SPIONs to customize their unique properties have made it possible to develop different types of SPIONs tailored for diverse functions/applications. More recently, considerable attention has been paid to the thermal effect of SPIONs for the treatment of diseases like cancer and for nanowarming of cryopreserved/banked cells, tissues, and organs. In this minireview, recent advances on the magnetic heating effect of SPIONs for magnetothermal therapy and enhancement of cryopreservation of cells, tissues, and organs are discussed, together with the nonmagnetic heating effect (i.e., high-intensity focused ultrasound or HIFU-activated heating) of SPIONs for cancer therapy. Furthermore, challenges facing the use of magnetic nanoparticles in these biomedical applications are presented. [DOI: 10.1115/1.4053007]

Keywords: magnetic nanoparticles, SPIONs, magnetothermal, hyperthermia, cancer, cryopreservation, nanowarming, HIFU

Introduction

Superparamagnetic iron oxide nanoparticles (SPIONs) have attracted a great deal of interest due to their unique properties such as their large surface area to volume ratio, easy manipulation with a magnet, high magnetization, and high saturation field [1–6]. The stability of SPION is affected by the balance of different attractive interactions such as magnetic, dipolar, and van der Waals interactions [7]. Therefore, bare SPIONs tend to aggregate together which affects their magnetic properties. To prevent this aggregation, they are often surface modified with protective shell(s) to stabilize them by either electrostatic or steric repulsion [8,9]. Therefore, SPIONs for biomedical applications often consist of a magnetic core and an outer organic layer which facilitates convenient functionalization to form SPION conjugates [10]. It is worth noting that magnetic nanoparticles can also perform as an energy transfer mediator and as a mechanical force vector. Therefore, through repeated alignments of magnetic spins and relaxations via processes of Néel rotation and Brownian motion in response to the alternating magnetic field, thermal energy can be generated from the magnetic nanoparticles [3,11–14].

Superparamagnetic iron oxide nanoparticles are mainly made of magnetite (Fe_3O_4) and maghemite (γ-Fe_2O_3) [15,16]. Different transition metal ions such as manganese [17], nickel [18], copper [19], and cobalt [20] can be mixed with the iron oxides to form SPIONs. The unique magnetic characteristics of SPIONs give them the ability to be rapidly heated upon exposure to an alternating current (AC) magnetic field, achieving a uniform heating throughout a large sample due to the large wavelength (at least a few meters) of the magnetic wave [21,22]. Therefore, magnetic induction heating is advantageous to traditional heating methods such as microwave oven or water-bath heating for which the heating is often heterogeneous and relies on thermal conduction [23–25].

This process, in which SPIONs are heated by an AC magnetic field (AMF) that is created by a few hundred (100–400 kHz) frequency AC passing through a solenoid coil, has quickly become an attractive method for various technological and biomedical applications [26,27]. When SPIONs are exposed to AMF inside the solenoid coil, there is a conversion of electromagnetic energy into thermal energy through the mechanisms of Brownian relaxation, Néel relaxation, and hysteresis losses [28–30]. The SPION heating efficiency is affected by the applied magnetic field frequency, nanoparticle size, nanoparticle anisotropy, and their collective behavior [31]. With their unique magnetic properties, SPIONs have been used in magnetic-based targeted drug delivery [32,33], cell differentiation [34,35], magnetic resonance imaging (as contrast agents) [36,37], biosensing [38–40], biological separation [41,42], and tissue engineering [43]. In this minireview, we will focus on the most recent use of SPIONs for heating in biomedical applications specifically in magnetothermal therapy [44], nanowarming of cells, tissues, and organs [45–47], and high-intensity focused ultrasound (HIFU)-mediated heating [48,49].

Magnetothermal Therapy

Magnetic induction heating is a noncontact method, for which an external magnetic field is applied throughout the sample that is

[1]Corresponding author.

Contributed by the Heat Transfer Division of ASME for publication in the Journal of Heat Transfer. Manuscript received September 1, 2021; final manuscript received November 3, 2021; published online January 18, 2022. Assoc. Editor: Ram Devireddy.

placed within a solenoid coil for heating [24,27]. This magnetic field is generated at frequencies typically below 30 MHz where the dielectric losses are negligible compared to resistive losses [50]. A transformer/generator is used for generating the desired AC current that is input into a solenoid coil to create an AC magnetic field in the coil (Fig. 1(*a*)) [14,51]. Under the AC magnetic field, heat may be generated within the SPIONs through mainly Néel and Brownian relaxations, together with hysteresis losses (Fig. 1(*b*)) [28–30,52].

Magnetothermal therapy is a type of thermal therapies, which uses the aforementioned magnetic induction heating for treating diseases like cancer. With this approach, a diseased tissue (e.g., tumor) is exposed to a magnetic field for heating to a high temperature (usually >43 °C) in the presence of magnetic nanoparticles, to kill diseased cells/tissues [53–56]. Studies have shown that high temperatures can result in irreversible damage to cancer cells in less than a minute to a few tens of minutes dependent on specific temperature and cell type [57–63]. The increase in temperature may lead to inactivation and denaturation of cellular proteins which may cause the dysfunction of cellular activities and eventually cell death [64–66]. Traditionally, cancer cells and tumors can be fatally heated through microwave (high-frequency electromagnetic wave) irradiation [67–69], optical laser irradiation [70,71], or ohmic heat generation [72–75]. However, due to the nonspecific nature of heating (for microwave and ohmic heating) and the limited tissue penetration depth of laser, these techniques are difficult to use for thermal therapy of deep-seated tumors, especially within the principal body cavities such as in the abdomen, thorax, and skull, often yielding recurrent tumor growth [24]. Another major disadvantage of traditional electromagnetic heating techniques is their nonspecific nature: both the diseased tissue and the neighboring healthy tissues may be heated directly [68,76], which may cause undesired dismal side effects if the healthy tissue performs critical functions. As a result, research has been focused on the use of targeted/specific thermal therapy methods to eliminate the cancerous cells by heating while minimizing damage to the surrounding healthy tissue.

One way to address the aforementioned challenge associated with conventional thermal therapies is magnetothermal therapy using SPIONs to convert the magnetic energy carried by the AC magnetic field into thermal energy, which can then increase the temperature in a well-defined area of the tumor containing the SPIONs [77,78]. This has been a major focus of studies regarding SPIONs for magnetothermal therapy of cancer. For example, Kossatz et al. synthesized functionalized SPIONs for targeted magnetothermal therapy in a breast cancer xenograft model [79]. Through a combination of a tumor-specific cell internalization moiety (N6L) and an anticancer drug (doxorubicin: DOX) on the SPIONs' surface, MDA-MB-231 breast cancer cells internalized the SPIONs and were then subcutaneously injected on the rear backside of the nude mice for hyperthermic treatment. The mice were exposed to a 435 kHz frequency AMF, generating hyperthermic temperatures in the tumor, which led to a 40% reduction in tumor volume, compared to the untreated control. However, despite the uniformity of the SPIONs in the tumor, maintaining hyperthermia inside the tumor remains a challenge due to different thermoregulatory conditions of the human body [80]. Therefore, factors that play important roles in SPIONs-mediated magnetic heating, such as the structural and magnetic properties of the SPIONs and the applied magnetic field, need to be further optimized [81].

A clinical study conducted by Dutz and Hergt concluded that the solenoid coil size can be optimized to generate an external magnetic field customized for the study [82]. When a small coil of 10 cm in diameter is used to generate an external magnetic field, patients were found to withstand the treatment for more than 1 h without any major discomfort if the product of AC amplitude and frequency of 5×10^9 A m^{-1} s^{-1} was not exceeded during magnetothermal therapy to minimize the eddy currents in healthy and/or in tumor tissue (which heats the normal and diseased tissue directly). A few years earlier, Johannsen et al., using an AMF

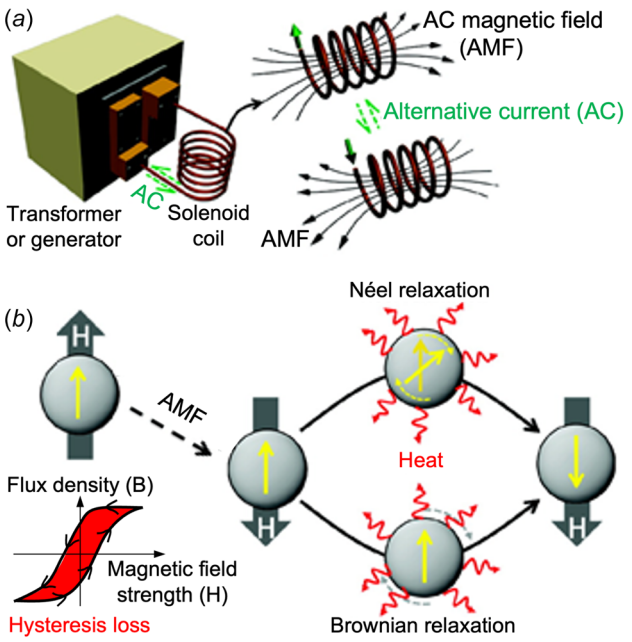

Fig. 1 Magnetic heating of SPIONs for magnetothermal therapy. (*a*) The induction heater consists of a transformer/generator to input an AC into a solenoid coil to generate an AMF for heating SPIONs. (*b*) A schematic illustration of the mechanisms of AMF heating of SPIONs. SPIONs perform as an energy transfer mediator and as a mechanical force vector. Through repeated alignments of magnetic spins and relaxations via Néel (spin rotation) and Brownian (particle rotation) relaxations, in response to the AC magnetic field, thermal energy can be generated from the magnetic nanoparticles. Heat can also be generated due to the hysteresis loss. (Reproduced with permission from Yoo et al. [14]. Copyright 2011 by American Chemical Society), with modification.

with a frequency of 100 kHz and a variable field strength ranging from 2.5 to 18 kA/m, tested SPIONs in ten prostate cancer patients [83]. Magnetothermal heating of SPIONs allowed the tissue to reach temperatures of up to 55 °C, resulting in a tumor reduction of up to 70%. However, this high temperature in the tumor due to the magnetic heating caused nonspecific heating to neighboring tissues (as a result of thermal diffusion) and localized discomfort in patients during magnetothermal treatments. SPIONs' biodistribution studies can also provide information on the effective design of a better system for magnetic heating. Pham et al. investigated the ex vivo biodistribution of two block copolymer-coated SPIONs in several organs of both healthy and sarcoma transplanted Swiss mice delivered via an intravenous injection [84]. They showed that many of the SPIONs accumulated in the liver while the least was found in the kidney after 24 h of SPION injection. The heating of the tumor was accomplished using a 5 kW power transformer or generator with an AC magnetic field of a 170–240 kHz, showing that a better heating is correlated to a higher SPION concentration.

Previous work has also focused on the modification of the physiochemical, structural, size, composition, and surface properties of the SPIONs to control the biodistribution, pharmacokinetics, and enhancing their heating efficiency at the tumor site [85–87]. Giustini et al. observed up to ~91% intracellular uptake of SPIONs after coating the nanoparticles with dextran [88]. Using sub-5 nm SPIONs, Wang et al. improved both the delivery and intratumoral distribution of these small SPIONs, demonstrating that they can easily extravasate from the tumor vasculature and readily diffuse into the tumor tissue [89]. This was followed by self-assembling in the acidic tumor micro-environment to limit their possibility of reentering the blood circulation. In this study, it was found that the improved passive targeting, intratumoral delivery, and

increased tumor retention of SPIONs are due to their easy extravasation into the tumor and restricted intravasation of clustered SPIONs. More recently, there has been an increasing interest in developing SPIONs that can be used for both magnetothermal therapy and magnetic resonance imaging of the tumor [90]. Du et al. developed an image-guided magnetothermal therapy using SPIONs to generate a well-distributed and high enough temperature to kill malignant tumor cells [91].

It is worth noting that intratumoral injection of SPIONs during magnetothermal therapy requires multiple injections at various sites of the tumor to increase SPION concentration and homogeneity of SPION distribution [92]. SPIONs were prepared and functionalized with CREKA (Cys–Arg–Glu–Lys–Ala), a pentapeptide that presents high affinity to fibrin–fibronectin complexes in the tumor, through a standard 1-ethyl-3-(3-dimethylamino propyl) carbodiimide hydrochloride/sulfo *N*-hydroxysuccinimide-coupling reaction [91]. SPIONs were synthesized and then intratumorally injected into orthotopic 4T1 tumor-bearing mice and placed under the AMF for hyperthermic treatment. The magnetic heating treatment was performed by applying an AMF at 400 kHz and 20 A for 10 min every 2 days for a total of three treatments. The functionalized SPIONs showed an improved targeting and SPION delivery uniformity, which resulted in a uniform increase of temperature and the total destruction of tumor. Intratumoral injection has been a preferred method for delivering SPIONs due to its ability to achieve a higher concentration of nanoparticles in tumor [93]. However, to improve tumor accumulation/retention and specificity, antibody/ligand conjugated SPIONs have been used to target various cancer-specific antigens for magnetothermal therapy [94,95]. For example, hyaluronic acid [96], trastuzumab [97], Herceptin [94], transferrin, and trans-activator of transcription (TAT,YGRKKRRQRRR) peptide [98] conjugated SPIONs have been used to target various receptors on tumor cells. Interestingly, magnetic heating of SPIONs is useful for not only hyperthermic applications but also in the low-temperature field as discussed in more details below.

Nanowarming

Long-term organ and tissue banking would revolutionize current approaches to transplantation and regenerative medicine by providing critical improvement to donor-to-donor organ supply and transport that would improve short- and long-term graft function [99–101]. Cryopreservation, a method used to preserve cell and tissues in a state of suspended animation at cryogenic temperatures (below −60 °C) for a considerable period of time [59,102], may provide better cell, tissue, and organ transplantation outcomes as well as an extended window for organ/tissue assessment, recovery, and allocation [99,101,103,104].

Fundamentally, cryopreservation can be categorized into (1) slow freezing, in which the biological samples are loaded into a low temperature-resistant container and cooled slowly (often at ~1-10 °C/min) to a low temperature usually between −40 °C and −80 °C before transferring into a liquid nitrogen (at −196 °C) tank for long-term storage [101,105,106], and (2) vitrification, in which biological samples are rapidly transformed from a liquid state into an amorphous glassy state through nonequilibrium cooling to minimize or eliminate ice formation [101,107,108]. Unlike slow freezing, the vitrification process requires a high cooling rate (as high as 10^6 °C/min depending on the CPA concentration) and often a high concentration (up to 5–8 M) of cryoprotective agents (CPAs) depending on the cooling rate used [108–110]. It is worth noting that to facilitate cryopreservation while minimizing different adverse effects that come with freezing (e.g., ice formation), CPAs like dimethylsulfoxide and small molecular sugars that affects the rate of water transport, ice nucleation, ice crystal growth, and the interactions between water/ice and biological materials are commonly used [104,111].

Vitrification has garnered much attention as a better alternative to slow freezing due to its ability to bypass the formation of ice crystals which may reduce/eliminate freezing-induced injury and improved cell survival [46,112,113]. For effective vitrification, the critical warming rate, needed to warm the organ back for transplantation, must exceed the respective critical cooling rate, the lowest rate that allows a solution to vitrify, by 1 to 3 orders of magnitude [114–116]. This is to ensure vitrification during cooling and avoid devitrification and/or recrystallization (which can lead to cell injury) during warming [117–119]. Unfortunately, it is difficult to achieve a high warming rate. For example, the overall warming rates achievable by the most commonly used heating in 37 °C water bath are only 10–100 °C min^{-1} depending on the sample size. Furthermore, the conventional water bath-based heating relies on thermal conduction from the boundary into the sample, which means nonuniform heating with large temperature gradient that creates thermal stress inside the sample, a major cause of mechanical damage to cryopreserved tissues and organs [120–122].

One potential solution to the challenges associated with the warming step of cryopreservation is SPION-based nanowarming. SPIONs can be used to achieve a relatively uniform distribution within tissues and organs due to their small nanoscale size, compared to micro- and macroscale tissues [123,124]. A combination of SPIONs and AMF of hundreds of kHz has generated a great interest in cryopreservation because it may provide uniform and rapid heating, which may reduce thermal–mechanical stresses and prevent devitrification/recrystallization during the warming phase of cryopreservation [46,121,125]. It is worth noting that SPIONs' heating under AMF is attributed to the dominant Néel relaxation mode and ferromagnetic hysteresis losses (Fig. 1(*b*)) [29,126].

Etheridge et al. presented a new approach for rapidly and uniformly warming a cryopreserved artery tissue sample of 1 ml via magnetic heating of SPIONs with an AMF of 20 kA/m at 360 kHz and 1 kW generated using a 2.75-turn water-cooled copper coil [21]. They demonstrated that heating rates as high as 300 °C/min could be generated with their SPION-based heating approach, which may minimize devitrification/recrystallization in the cryopreserved biospecimen. Moreover, Wang et al. looked at the effect of magnetic heating of SPIONs on cryopreservation of 200 μl of suspension of human umbilical cord matrix mesenchymal stem cells loaded in a plastic straw by vitrification (Fig. 2(*a*)) [125]. They found that magnetic heating of SPIONs can improve the heating rate during warming the cell sample, resulting in significantly improved cell viability postwarming. Further studies have shown that the cryopreserved cells can retain their stemness and functional capability of multilineage differentiation after warming. Of note, it is essential to employ SPIONs that are colloidally stable to maintain their heating ability. To improve stability and minimize aggregation of SPIONs in suspension, Gao et al. synthesized silica-coated SPIONs [128]. In this study, the authors introduced 10 mg Fe ml^{-1} of SPIONs suspended in the VS55 solution, a widely used vitrification solutions with a high concentration of CPAs for vitrification, in a stepwise manner into the rat kidney through the kidney infrarenal aorta. The vitrified biospecimen in a 1.75 ml Eppendorf tube was magnetically warmed in a 2.75-turn copper coil at 20 kA m^{-1}, 360 kHz, and 1 kW, to create a warming rate of 130 °C min^{-1}. The results showed a 85.3% kidney cell viability after the magnetic nanowarming despite a heterogeneous distribution of the SPIONs in the biospecimen.

Subsequently, Manuchehrabadi et al. designed a system that demonstrates that SPIONs-mediated heating can improve the viability of tissue and prevent physical failure during cryopreservation of 1–80 ml of samples of cryopreserved porcine arterial and heart valve tissues [46]. Coupling of a relatively low radio frequency AC (60 kA/m alternating at 175 kHz on a 15 kW radio frequency system) magnetic field and mesoporous silica-coated SPIONs was employed to rapidly heat porcine carotid tissue samples after vitrification. In this study, silica-coated SPIONs were dispersed in CPA solutions before the AMF heating was used to enable highly uniform and rapid heating of the vitrified sample. After cooling and warming back, the viabilities of the sample with

nanowarming (~90 °C/min) were found to be much higher than that with conventional water-bath heating (~7 °C/min). To achieve a high energy conversion while reducing the SPION dosages, Pan et al. designed an electromagnetic warming system in which low concentrations of SPIONs were added into the CPA solution [129]. They reported the addition of SPIONs generated rapid warming of the bulk cryopreserved sample at >200 °C min^{-1}. Chiu-Lam et al. synthesized polyethylene glycol (PEG)-coated SPIONs that are stable in the VS55 solution for cryopreservation by vitrification and used them for nanowarming of vitrified whole rat hearts [103]. In their study, they reported that these PEG-coated SPIONs can achieve high warming rates of up to 321 °C/min under an AMF of 42.5 kA/m alternating at 278 kHz. The SPIONs can be successfully perfused uniformly into the whole rat heart and be efficiently washed-out using histidine–tryptophan–ketoglutarate solution after cooling, cryostorage in liquid nitrogen, and nanowarming. It is worth noting that despite efficient heating of the SPIONs, cells that are in their proximity may have the risk of overheating [83,130–132], and some studies have reported on the toxicity of high concentrations of SPIONs to the neighboring cells [133,134].

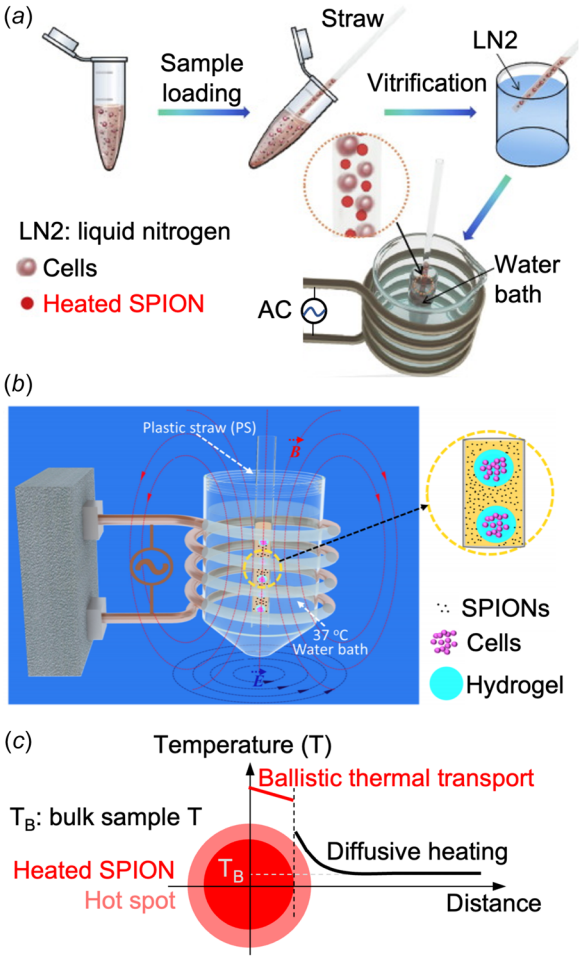

Fig. 2 Magnetic heating of SPIONs for nanowarming. (*a*) A schematic illustration of the procedure of preparing human umbilical cord matrix mesenchymal stem cells for cryopreservation by vitrification using a plastic straw with SPION-mediated magnetic induction heating for warming, (*b*) A schematic illustration of using hydrogel micro-encapsulation of cells to eliminate direct contact between cells and SPIONs for warming the cryopreserved hydrogel-cell constructs, and (*c*) A schematic illustration of the hot spot generated around a SPION during magnetic heating, due to ballistic thermal transport within the nanoparticle and Fourier diffusive heating in the adjacent medium. The sketches in (*a*) and (*b*) are reproduced with permission from Wang et al. [125] (Copyright 2016 Acta Materialia Inc. by Elsevier) and Liu et al. [127] (Copyright 2018 by American Chemical Society), respectively, with modification.

To overcome this challenge, recent studies have focused on developing systems in which cells do not have any direct physical contact with the SPIONs [127,135]. In these studies, SPIONs are suspended in the CPA solution outside the alginate hydrogel-cell constructs (Fig. 2(*b*)). Stem cells can be encapsulated inside the alginate hydrogel construct and avoid physical contact with the SPIONs to eliminate their potential toxicity, if any, to the cells. After nanowarming with SPIONs under an AMF generated by a 6-turn coil at 375 kHz, >80% cell survival was observed for encapsulated stem cells, due to the protection of the cells from ice crystal formation by the alginate hydrogel and nanowarming. This was in contrast to the <27% cell survival for nonencapsulated cells where most of the cells were killed by ice formation (i.e., devitrification/recrystallization) during conventional warming with a water bath. It is worth noting that the mechanisms of nanowarming on inhibiting devitrification/recrystallization during warming may be attributed to both the global (due to Fourier diffusive heating in the cryopreservation solution) and local (due to ballistic heating within the SPIONs) inhibition mechanisms (as illustrated in Fig. 2(*c*)). The former is due to the enhanced overall warming rate of the entire sample to surpass the critical warming rate for inhibition of devitrification (via suppression of nucleation) and/or ice recrystallization (via suppression of both nucleation and growth) globally in the entire sample during warming. The latter is due to the thousands to millions and billions (depending on the concentration of SPIONs in the sample) discrete hot spots adjacent to the SPIONs in the sample, which may inhibit ice formation (mainly via suppression of ice nucleation) locally since ice nucleation is also a discrete stochastic event [101]. Magnetic heating of the SPIONs to generate hotspots in the vicinity of the SPIONs is possible, because the size of the SPIONs is similar to the mean free path of the materials in them, leading to ballistic thermal transport in the nanoscale particles that is much less efficient than the Fourier conduction/diffusion of heat in bulk materials [136–141].

Superparamagnetic iron oxide nanoparticles-embedded hydrogels has also been used to suppress ice formation in combination with other heating mechanisms for enhanced warming. Cao et al. made alginate-based hydrogel constructs with embedded graphene oxide (GO)–Fe_3O_4 nanocomposites capable of inhibiting ice recrystallization by infrared irradiation that generates heat via GO and magnetic field for generating heat via Fe_3O_4 [142]. They evaluated both the photothermal and magnetothermal effects of stem cell-laden hydrogel constructs under near-infrared laser and AMF. Further studies showed that after warming, stem cells inside the hydrogel retain their original structure with high viability (>80%) after long-term culture (7 days).

Superparamagnetic iron oxide nanoparticle-based nanowarming has demonstrated the potential to be a revolutionary technology for the field of cryopreservation, which is invaluable for cell, tissue, and organ banking. The SPIONs-based magnetothermal effect has also been utilized in other biomedical areas such as glucose regulation [143,144]. For instance, Stanley et al. decorated a modified temperature-sensitive channel, TRPV1, with antibody-coated SPIONs which were heated with a low-frequency magnetic field to regulate the protein production [145]. In this study, the heating of SPIONs led to an increase in temperature rise at the TRPV1 calcium gate, which subsequently led to the synthesis and release of insulin to lower the blood glucose level in mice. Interestingly, SPIONs not only can be heated by magnetic field but also others like the acoustic field with mechanical wave as summarized below.

Enhancement of High-Intensity Focused Ultrasound Heating

High-intensity focused ultrasound is a minimally invasive ablation technique that uses both heat and acoustic cavitation to

destroy diseased cells and tissues including tumors [146–148]. HIFU-mediated heating is comprised of two major elements as shown in Fig. 3: an ultrasound generator and a piezoelectric transducer [149]. The operating mechanism centers around the generation of a focused ultrasound field by the piezoelectric transducer. This transducer is able to generate ultrasound waves with a frequency ranging from 1 to 7 MHz [150]. The acoustic energy is generated and detected using piezoelectric crystals that function as an interface between electrical and mechanical energy [151]. These ultrasound waves can travel through the tissue and converge at one focal area, where their energy is converted into thermal energy. The temperature at the focal area could reach more than 60–95 °C within seconds, causing instantaneous cell death [48]. It is worth noting that an additional coupling medium such as water is placed in between the transducer and the target tissue surface to minimize acoustic loss [152]. The HIFU beam focusing minimizes the possibility of thermal damages to nontargeted tissue [153]. For this reason, it has emerged as a promising technology that can be employed as either a standalone treatment method or an adjuvant method that can enhance the effectiveness of other available treatments due to its noninvasive nature [154,155].

However, despite its great potential in clinical treatments of various cancers (e.g., breast [156], kidney [157], liver [158], and prostate [159] cancers, together with soft tissue sarcoma [160]), there have been many challenges in using acoustic energy for tumor treatment [48,161]. The assumption that there is a linear attenuation of the acoustic energy in the soft tissues between the transducer and the target might not always be accurate because the soft tissues are heterogeneous and might attenuate acoustic energy differently [162,163]. This has led to unablated cells in certain areas of the tumor as well as damage to normal tissue due to high acoustic power [164]. Furthermore, due to the high level of acoustic energy required during HIFU for ablating a large tumor, skin burns and other adverse effects stemming from high acoustic energy and long sonication time such as overheating of surrounding healthy tissue have been observed in a few studies [165,166].

To overcome these challenges, various exogenous absorbers such as porphyrin, xanthene, and microbubbles that can enhance the thermal ablation by increasing the attenuation and dissipation of acoustic energy, leading to lower ultrasound power, have been explored [161,167]. More recently, SPIONs have emerged as effective sonosensitizers for focused ultrasound therapy [30]. SPIONs increase the attenuation of the acoustic wave within the local tumor area, which may lead to the heating by the ultrasound while sparing the surrounding healthy tissues [168]. For this reason, they have been used to facilitate and enhance HIFU thermal ablation.

Ho et al. investigated the advantages of SPIONs in combination with HIFU to destroy HeLa multicellular tumor spheroids [169]. The HIFU transducer was operated with a frequency of 1.1 MHz, pulse repetition frequency of 1.67 kHz, and peak negative focal pressure of 7.2 MPa for 10 s. After exposing the cells to both SPIONs and HIFU, there was a significant increase in the HIFU induced inertial cavitation which led to the enhancement of the rate of destruction of tumor spheroids. Subsequently, Ahmad Reza Dibaji et al. used SPIONs to locally enhance heating at low powers during HIFU ablation [170]. In this study, the transducer with a focal length of 6.26 cm, an inner diameter of 2.2 cm, and an outer diameter of 6.4 cm operating at a frequency of 1.025 MHz was used to test various SPIONs' concentrations (0% as control, 1%, and 3% w/v) at three distinct acoustic powers (5.2, 9.2, and 14.3 W), which showed a high thermal dose could be achieved even at a low acoustic power when the SPION concentration is high. They found that when SPIONs are used, the required HIFU power to obtain an efficient thermal dose that can cause cell necrosis in tumors can be reduced substantially.

More recently, Devarakonda et al. examined the temperature rise, thermal dose, and the lesion volume of tumor after HIFU with/without SPIONs [164]. Using different SPION concentrations (0% for control, 0.0047%, and 0.047% w/v) that are at least 20 times lower than those previously used in the literature [170], they found that by using only 0.047% SPIONs to enhance HIFU ablation, it was possible to decrease the power required to obtain a tumor lesion volume of 13 mm^3 by half. Kaczmarek and coworkers assessed the utility of SPIONs in ultrasound hyperthermia by enhanced heating in low-power ultrasound [168,171]. SPIONs with various concentrations (0.26–0.35% w/w) were used. The acoustic power of the transducer was set to 2.5 W with a frequency of 1 and 3.5 MHz. It was found that the simultaneous use of the SPIONs and HIFU leads to a synergistic increase of temperature during ultrasound heating and enabled more precise control over the heating process. In an effort to investigate the heating process of SPION-enhanced HIFU, Sadeghi-Goughari et al. used

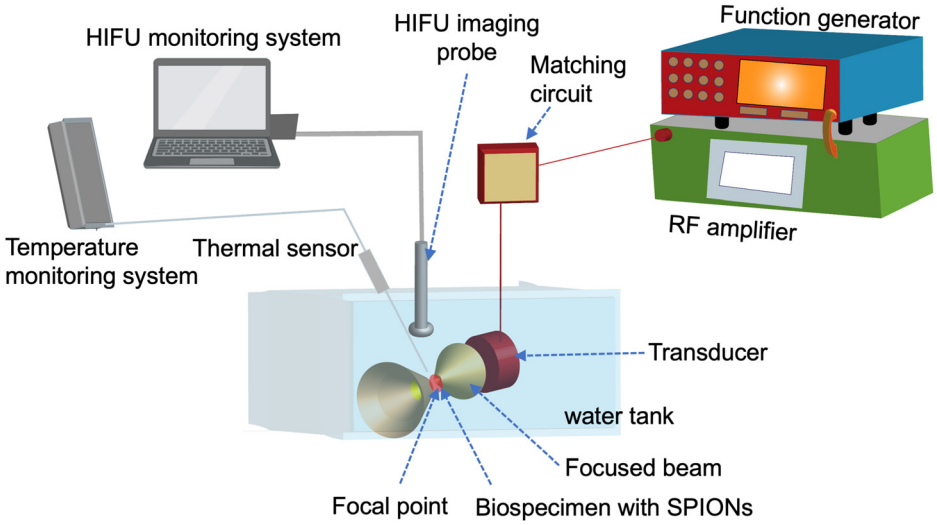

Fig. 3 HIFU heating of SPIONs-laden biospecimen. An HIFU system is comprised of a function generator, a gain-variable power amplifier, a transducer, a water tank, an HIFU imaging probe, and a thermal sensor. The transducer creates an ultrasound beam which is focused to a focal point in the target tissue. The kinetic energy of the ultrasound beam is converted into thermal energy, which may cause instantaneous damage to diseased cells and tissues. This heating process may be enhanced by using SPIONs delivered in the biospecimen.

Table 1 A summary of the various types of SPIONs together with the methods of their synthesis and the major results of their use for the three biomedical applications discussed in this review 179185MnFe2O4@ CoFe2O4

Type	Synthesis method	Major result	Reference
	Magnetothermal therapy		
MF66 MNP	Coprecipitation of Fe^{2+} and Fe^{3+} followed by dimercaptosuccinic acid stabilization	Magnetic hyperthermia of breast cancer led to a 40% tumor reduction	[79]
Magforce nanoparticles	Magforce AG (Berlin, Germany) company	Thermal therapy of cancer tumor	[83]
Copolymer-coated Fe_3O_4 nanoparticles	Coprecipitation of Fe^{2+} and Fe^{3+} followed by polystyrene-copolyacrylic acid, polylactide acid, and polyethylene glycol coating	Magnetic inductive heating of organs of mouse models	[84]
mPEG-coated Fe_3O_4 nanoparticles	Solution-phase thermal decomposition of $Fe(acac)_3$ in oleic acid and benzyl ether	High-performance magnetic hyperthermia	[85]
Anionic iron oxide nanomagnets	Alkaline coprecipitation of iron (III) and iron salts followed by citrate stabilization	Colloidal mediators for magnetic hyperthermia	[86]
Oxide nano-octopods	Nonhydrolytic thermal decomposition of $Fe(acac)_3$ in the presence of oleic acid and oleylamine	Magnetic hyperthermia treatment	[87]
Cys–Arg–Glu–Lys–Ala modified magnetic ferrite nanoparticles	High-temperature thermal decomposition of $Fe(acac)_3$ in the presence of oleic acid	Combined hyperthermia and MRI/magnetic particle imaging of malignant tumor	[91]
Magnetic multicore nanoparticles	Coprecipitation of Fe^{2+} and Fe^{3+} followed by carboxymethyl dextran coating	Tumor heating within 60 s	[175]
Water-dispersible sugar-coated iron oxide nanoparticle	Thermal decomposition of $Fe(acac)_3$ followed by sugar coating	Relaxometry and magnetic hyperthermia	[176]
AEH–Fe_2O_3 nanomagnetic beads	Magnetic iron oxide particles encapsulated within a coating formed from a polyester of valeric and butyric acids	Treated tumors decreased in volume by 50–94%	[177]
PVP coated magnetoplasmonic nanoparticles	Coprecipitation of Fe^{2+} and Fe^{3+} followed by gold seeding	Photothermia with magnetic hyperthermia of cancer	[178]
$CoFe_2O_4$@$MnFe_2O_4$	Thermal decomposition of $MnFe_2O_4$ onto the surface of $CoFe_2O_4$	Antitumor therapeutic heating	[44]
$Zn_{0.4}Fe_{2.6}O_4$ MNP	Magnetic nanoparticles are coated with SiO_2 and then amine-functionalized with geldanamycin	Resistance-free apoptotic hyperthermia	[179]
Fe_3O_4 nanoparticles	Oxidation of pentacarbonyl iron followed by purification process	Selective inductive heating of lymph nodes	[180]
Biomimetic magnetic nanoparticles	The precipitation of inorganic magnetite, followed by an oxidation of a strong base (NaOH)	Targeted magnetic hyperthermia	[181]
Magnetosome chains	Extracted from magnetotactic bacteria	Efficient penetration and maximum cell destruction	[182]
DOX/PLGA-Fe MNP	Dispersion of Fe powder into DOX/PLGA solution by stirring	Chemomagnetic-hyperthermia-induced synergistic tumor eradication	[183]
Oleic acid functionalized Fe_3O_4	Coprecipitation of $FeSO_4$ and $FeCl_3$ followed by NH_4OH	Tumor growth inhibition by apoptosis and Hsp90/AKT modulation	[184]
mAb-guided bioprobes	Polyethylene glycol–iron oxide-impregnated dextran nanoparticles functionalized with dodecanetetraacetic acid	Thermoablative therapy for human breast cancer in mice results in tumor reduction	[95]

Table 1 (continued)

Type	Synthesis method	Major result	Reference
PEGylated Mn–Zn ferrite nanocrystals	Thermal decomposition of $Fe(acac)_3$ in presence of $Zn(acac)_2$ and manganese (II) acetylacetonate followed by oleylamine coating	Induce the apoptosis of tumor cells, inhibit the angiogenesis of tumor vessels, and suppress the tumor growth	[185]
Iron oxide nanocubes	Thermal decomposition of $Fe(acac)_3$	Magnetic hyperthermia and photothermal bimodal treatment leading to a complete apoptosis-mediated cell death	[186]
Poly (D, L-lactic-coglycolic acid) encapsulated SPIONs	Chemical coprecipitation of Fe^{3+} and Fe^{2+} in ammoniacal medium followed by solvent evaporation for encapsulation	Cancer destruction within a short period of time (120 min) by initiating early and late apoptosis	[187]
Magnetic iron oxide nanoparticles	Thermal decomposition of $Fe(acac)_3$ in a mixture of oleic acid, oleylamine, and long acyl chain diols in benzyl ether	Effectively heat tumor tissues at a minimal dose	[188]
	Nanowarming		
Ferrotec EMG308 solution	Fe_3O_4 nanoparticles coated with an anionic surfactant in aqueous suspension	Thawing of a cryopreserved artery tissue sample	[21]
Silica-coated EMG308, Ferrotec/silica-coated iron-oxide nanoparticles	EMG308, Ferrotec nanoparticles coated with mesoporous silica	Thawing cryopreserved porcine arterial and heart valve tissues with improved viability	[46]
PEG-coated SPIONs	chemical coprecipitation of Fe^{3+} and Fe^{2+} followed by PEG coating	Successful perfusion of vitrified whole rat hearts	[103]
Fe_3O_4 nanoparticles	Chemical coprecipitation of Fe^{3+} and Fe^{2+} followed by aqueous ammonia mixture	Significantly facilitates rewarming and improves the cryopreservation outcome of human umbilical cord matrix mesenchymal stem cells	[125]
Amine group functionalized Fe_3O_4	Fe_3O_4 nanoparticles purchased from Ocean Nanotech LLC, San Diego, CA	Rewarming of bulk sample	[129]
Fe_3O_4 NPs	Chemical coprecipitation of Fe^{3+} and Fe^{2+}	Low-cryoprotectant vitrification of stem cell-alginate hydrogel construct	[127]
Fe_3O_4 NPs	Chemical coprecipitation of Fe^{2+} and Fe^{3+} ions	Massive-volume vitrification of stem cells with low-concentration cryoprotectants	[135]
GO–Fe_3O_4 nanocomposites	GO is added to the mixture of acetate stabilized Fe_3O_4	Inhibit ice recrystallization by infrared irradiation that generates heat via GO and magnetic field for generating heat via Fe_3O_4	[142]
DP6 + silica-coated iron-oxide nanoparticles	Fe_3O_4 nanoparticles coated with a silica layer and functionalized with polyvinyl pyrrolidone	Warming of cryopreserved sample	[189]
Mesoporous silica-coated Fe_3O_4 nanoparticles	PVP coated nanoparticles are coated with silica shell followed by stabilization of PEG–TMS	Nanowarming of a cryopreserved rat kidney infrarenal aorta with preserved morphology and good viability at the cellular level	[190]
CP-DMSA-MNPs	Chemical coprecipitation of Fe^{2+} and Fe^{3+} ions followed by dimercaptosuccinic acid coating	Multihot-spot induction and sequential regulation	[191]
TD-PMAO-MNPs	Thermal decomposition of $Fe(acac)_3$ followed by polymaleic anhydride-alt-1-octadecene coating	Multihot-spot induction and sequential regulation	
OP-PAA-MNPs	Oxidative precipitation of $FeSO_4$ by NaOH followed by	Multihot-spot induction and sequential regulation	

Table 1 (continued)

Type	Synthesis method	Major result	Reference
	a coating of polyacrylic acid		
Magnetoliposomes	Surrounding the iron oxide nanoparticles (Fe_3O_4) with phospholipid bilayer	Magnetic fluid hyperthermia efficacy on pancreatic tumor cell reached 95% tumor cell death	[192]
	HIFU-activated heating		
MNPs	Not available (purchased from U.S. Research Nanomaterials, Inc., Houston, TX)	NPs play the major role in the temperature rise during HIFU sonication	[161]
Magnetic nanoparticles	Purchased as EMG705 series, Ferrotec (Tokyo, Japan)	Reduced damage to healthy tissue, and reduced the procedure time, during tumor ablation using HIFU	[164]
Magnetite (Fe_3O_4) nanoparticle agglomerates	Chemical coprecipitation of Fe^{2+} and Fe^{3+} ions with ammonia solution	Magnetite nanoparticle agglomerates enhance the efficacy of HIFU in destruction of tumor spheroids	[169]
Magnetic nanoparticles (Fe_3O_4))	Purchased as EMG705 series, Ferrotec	Significantly reduce the time for HIFU thermal ablation	[170]
SPION	Chemical coprecipitation using ferric and ferrous salts in alkali medium followed by sodium oleate coating	The presence of SPION increases the absorption of ultrasound energy leading to increased temperature	[171]
Multifunctional PFH/DOX@PLGA/Fe_3O_4-Folic acid nanocomposites	Double-emulsion	Demonstrated to efficiently suppress the tumor growth based on the enhanced and synergistic chemotherapy and HIFU ablation	[172]
Superparamagnetic PLGA–iron oxide microcapsule	Double-emulsion (water/oil/water) evaporation process	Dual-modality ultrasound /MR imaging and high-intensity focused U.S. breast cancer ablation	[173]
Ultrasmall superparamagnetic iron oxide/PLGA microspheres	A double-emulsion evaporation method was used to synthesize ultraminiature superparamagnetic PLGA–iron oxide microcapsules	Significantly enhance dual-modality ultrasound/MR imaging and HIFU synergistic therapy with an intravenous administration method	[174]

AEH: arterial embolization hyperthermia, mPEG: methoxy polyethylene glycol, acac: acetylacetonate, PVP: polyvinyl pyrrolidone, GO: graphene oxide, TMS: trimethyl (TM) and succinimide ester, DMSA: dimercaptosuccinic acid, PMAO: polymaleic anhydride-alt-1-octadecene, PAA: polyacrylic acid, CP: chemical coprecipitation, TD: thermal decomposition, and OP: oxidative precipitation.

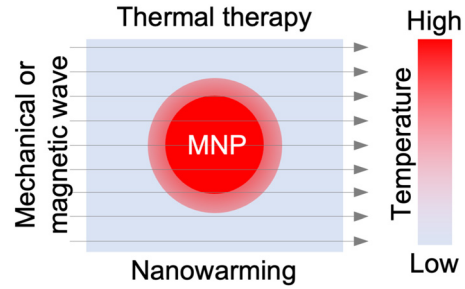

the principle of conservation of energy for heat transfer mechanism to derive a set of HIFU equations that govern the temperature variation during thermal ablation [161]. In this study, a numerical model was developed to simulate the absorption mechanism of HIFU in the presence of SPIONs which leads to the temperature rise during the sonication period. Moreover, a series of experiments were performed to verify the accuracy of the model. They found that the temperature rise during HIFU sonication emanates from the transport process that takes place at the boundaries between SPIONs and the surrounding medium. Additionally, they reported that the effects of SPION heating can be improved by amplifying the acoustic power and the SPION concentration.

With their multifunctional properties, SPIONs can also be used as contrast agents for both HIFU and magnetic resonance imaging [172]. Sun et al. successfully integrated SPIONs into poly(lactic-coglycolic acid) (PLGA) microcapsules to simultaneously enhance ultrasound cancer imaging and the HIFU ablation in a rabbit-bearing breast cancer model [173]. Shortly after, Zhou et al. developed PLGA–SPION microspheres for dual imaging and HIFU ablation of liver tissue in rabbits [174]. The focal length of the piezoelectric transducer in this study was 145 mm with a diameter of 220 mm and an operating frequency of 0.94 MHz, while a 3.5–5 MHz ultrasound transducer was applied for imaging. The PLGA–SPION microspheres were introduced through intravascular injection followed by HIFU ablation. The targeted tissue was then subjected to pathological examination to determine its structural changes. The results showed that PLGA–iron oxide microsphere could enhance ultrasound imaging and efficiently enhance HIFU ablation of liver tissue in rabbits. Given these findings, the use of SPIONs during HIFU tumor ablation has the potential to reduce damage to healthy tissue and lower the HIFU power needed to destroy tumors. Moreover, magnetic resonance imaging, when combined with HIFU, would provide image guidance by identifying tumors for targeting and for tracking the ablation lesion with greater resolution.

Summary and Outlook

In this minireview, different biomedical applications of SPION-based heating and their respective mechanisms are discussed. A summary of the various types of SPIONs together with the methods of their synthesis and the major results of their use for the three different biomedical applications discussed in this work is given in Table 1. The future of SPION-based magnetic induction heating in biomedical applications truly holds great potential, especially in cancer therapy and in nanowarming/cryopreservation of cells, tissues, and organs. To date, magnetic heating has been explored to treat many different malignancies [193,194]. However, despite progress made to achieve efficient magnetic heating of SPIONs and use it in both therapeutic and cryopreservation applications, there is still more work that needs to be done to fully integrate these methods in a clinical setting. Different studies and reports have shown that magnetic heating of SPIONs depends not only on their size and other physical properties but also on the frequency and power used during the process. For these reasons, it is imperative to standardize and establish a clinically acceptable SPION size, composition, shape, and surface-functionalization that can be acceptable for clinical applications. Moreover, the nonuniformity of the magnetic field and the difference in its absorption and dissipation by different tissues in organs have proven to be a hurdle in generating a uniform warming [128]. Therefore, a standardized frequency and power appropriate for efficient magnetic heating need to be established.

Furthermore, there is still difficulty in synthesizing SPIONs with special properties such as negligible cellular uptake and cellular association, which would allow their maximum removal after nanowarming for cryopreservation applications. Hence, further studies are needed to generate SPIONs that are colloidally stable to maintain their heating potential while being able to be perfused in and out of the vasculature of the tissue/organ conveniently. Certain hurdles such as the overheating of SPIONs that lead to the destruction of neighboring tissues have also been raised [76]. However, this can be avoided by functionalizing the SPIONs with targeting moieties which allow them to bind to the target only for increasing the SPIONs' localization to the targeted tissues/cells before applying the magnetic field [16,78].

Additional technologies in which external energy (e.g., near-infrared laser radiation) is coupled to the SPIONs to increase intratumoral temperatures should be explored more [195]. The combination of therapy and diagnostics (theragnostic) including the combination of HIFU and SPIONs has garnered significant attention due to their ability to introduce a targeted treatment and monitor the response to the therapy. Moreover, the simultaneous use of the SPIONs and HIFU has proven very efficient in reducing the amount of acoustic power necessary for the tissue targeting while enhancing the heating at the local region of the tumor and allowing more precise control over the heating process.

Despite this feat, the use of HIFU–SPIONs mediated heating has been developing relatively slower than other applications such as MRI, or magnetothermal therapy. Even though HIFU is a U.S. Food and Drug Administration (FDA)-approved method for the treatment of various diseases [196–199], there are still challenges that are associated with the use of SPIONs. These include the effective delivery of stable SPIONs into the target area of the tumor. The tumor micro-environment contains different barriers, such as a thick stroma, high interstitial fluid pressure, and macrophage uptake that might hinder the efficient and uniform accumulation of the SPIONs into a tumor [200,201]. Additionally, unlike the leaky vasculature in mouse models that grow fast, the vasculature of human tumor with a slow growth rate may not be as leaky, which might limit SPION accumulation into the tumor [202]. Therefore, more advanced models that can better recapitulte human tumors or clinical studies on humans are needed to further advance this technology. Other new techniques and methods that combine both magnetic heating and imaging should be explored to facilitate more targeted heating via guidance by imaging for therapeutic applications [91,203,204]. Recently, new emerging technologies such as artificial intelligence may be used to predict the efficiency of SPIONs' heating based on their size, composition, and frequency before the actual use [205]. This technology may also be used to design and optimize different types of SPIONs, or other magnetic nanoparticles customized for different medical uses [206,207].

It is worth noting that with the increasing biomedical applications of SPIONs, there has been also an increase in public concerns about their biosafety, long-term biodistribution, and clearance from the body. However, these concerns have been assuaged by a few recent FDA approvals of SPION-based nanomedicines for human use. These include Feraheme® (ferumoxytol), a nonstoichiometric polyglucose sorbitol carboxymethyl ether capped SPION used for the treatment of iron deficiency associated with chronic kidney disease [208], together with ferumoxtran-10, ferucarbotran (Resovist®), and Feridex® (ferumoxides) which are approved for use as magnetic resonance imaging contrast agents [209]. These recent FDA approvals cement the biosafety of SPIONs and their efficacy in treating different diseases. It is anticipated that more SPIONs' formulations will be developed and used soon for different biomedical applications. This may include SPION-based treatment of diseases in hard-to-reach deep organs (e.g., glioblastoma multiforme and Parkinson's and Alzheimer's diseases in the brain) [210,211]. Furthermore, SPION-based nanowarming studies so far have been focused on smaller samples. Scaling this technology to larger samples like organs (e.g., heart, liver, and lung) would provide a game-changing and lifesaving technology in the organ transplantation field.

Acknowledgment

The authors would like to acknowledge the support from the National Institutes of Health as detailed in the Funding Data section below.

Funding Data

- National Institutes of Health (R01EB023632; Funder ID: 10.13039/100000002).
- National Institutes of Health (R01CA206366; Funder ID: 10.13039/100000002).
- National Institutes of Health (R01CA243023; Funder ID: 10.13039/100000002).

References

[1] Kodama, R. H., 1999, "Magnetic Nanoparticles," J. Magn. Magn. Mater., **200**(1–3), pp. 359–372.
[2] Wu, W., He, Q., and Jiang, C., 2008, "Magnetic Iron Oxide Nanoparticles: Synthesis and Surface Functionalization Strategies," Nanoscale Res. Lett., **3**(11), pp. 397–415.
[3] Kwizera, E. A., Chaffin, E., Shen, X., Chen, J., Zou, Q., Wu, Z., Gai, Z., 2016, "Size- and Shape-Controlled Synthesis and Properties of Magnetic-Plasmonic Core-Shell Nanoparticles," J. Phys. Chem. C, **120**(19), pp. 10530–10546.
[4] Kwizera, E. A., Chaffin, E., Wang, Y., and Huang, X., 2017, "Synthesis and Properties of Magnetic-Optical Core-Shell Nanoparticles," RSC Adv., **7**(28), pp. 17137–17153.
[5] Afzalipour, R., Khoei, S., Khoee, S., Shirvalilou, S., Raoufi, N. J., Motevalian, M., and Karimi, M. Y., 2021, "Thermosensitive Magnetic Nanoparticles Exposed to Alternating Magnetic Field and Heat-Mediated Chemotherapy for an Effective Dual Therapy in Rat Glioma Model," Nanomedicine, **31**, p. 102319.
[6] Kharat, P. B., Somvanshi, S. B., Khirade, P. P., and Jadhav, K. M., 2020, "Induction Heating Analysis of Surface-Functionalized Nanoscale $CoFe_2O_4$ for Magnetic Fluid Hyperthermia Toward Noninvasive Cancer Treatment," ACS Omega, **5**(36), pp. 23378–23384.
[7] Appel, C., Kuttich, B., Kraus, T., and Stuhn, B., 2021, "In Situ Investigation of Temperature Induced Agglomeration in Non-Polar Magnetic Nanoparticle Dispersions by Small Angle X-Ray Scattering," Nanoscale, **13**(14), pp. 6916–6920.
[8] Gutierrez, L., de la Cueva, L., Moros, M., Mazario, E., de Bernardo, S., de la Fuente, J. M., Morales, M. P., and Salas, G., 2019, "Aggregation Effects on the Magnetic Properties of Iron Oxide Colloids," Nanotechnology, **30**(11), p. 112001.
[9] Kalambur, V. S., Longmire, E., and Bischof, J. C., 2007, "Characterization of Cell Association and Heat Treatment Using Iron Oxide Magnetic Nanoparticles," ASME Paper No. SBC2007-176216.
[10] Frey, N. A., Peng, S., Cheng, K., and Sun, S., 2009, "Magnetic Nanoparticles: Synthesis, Functionalization, and Applications in Bioimaging and Magnetic Energy Storage," Chem. Soc. Rev., **38**(9), pp. 2532–2542.
[11] Williams, H. M., 2017, "The Application of Magnetic Nanoparticles in the Treatment and Monitoring of Cancer and Infectious Diseases," Biosci. Horiz.: Int. J. Stud. Res., **10**, p. hzx009.
[12] Vaishnava, P. P., Tackett, R., Dixit, A., Sudakar, C., Naik, R., and Lawes, G., 2007, "Magnetic Relaxation and Dissipative Heating in Ferrofluids," J. Appl. Phys., **102**(6), p. 063914.
[13] Dutz, S., and Hergt, R., 2014, "Magnetic Particle Hyperthermia—A Promising Tumour Therapy?," Nanotechnology, **25**(45), p. 452001.
[14] Yoo, D., Lee, J. H., Shin, T. H., and Cheon, J., 2011, "Theranostic Magnetic Nanoparticles," Acc. Chem. Res., **44**(10), pp. 863–874.
[15] Hosono, T., Takahashi, H., Fujita, A., Joseyphus, R. J., Tohji, K., and Jeyadevan, B., 2009, "Synthesis of Magnetite Nanoparticles for AC Magnetic Heating," J. Magn. Magn. Mater., **321**(19), pp. 3019–3023.
[16] Wahajuddin, M., and Arora, S., 2012, "Superparamagnetic Iron Oxide Nanoparticles: Magnetic Nanoplatforms as Drug Carriers," Int. J. Nanomed., **7**, pp. 3445–3471.
[17] Zipare, K., Dhumal, J., Bandgar, S., Mathe, V., and Shahane, G., 2015, "Superparamagnetic Manganese Ferrite Nanoparticles: Synthesis and Magnetic Properties," J. Nanosci. Nanoeng., **1**(3), pp. 178–182.
[18] Deb, P., Basumallick, A., and Das, S., 2007, "Controlled Synthesis of Monodispersed Superparamagnetic Nickel Ferrite Nanoparticles," Solid State Commun., **142**(12), pp. 702–705.
[19] Tajik, S., Beitollahi, H., Aflatoonian, M. R., Mohtat, B., Aflatoonian, B., Shoaie, I. S., Khalilzadeh, M. A., 2020, "Fabrication of Magnetic Iron Oxide-Supported Copper Oxide Nanoparticles (Fe_3O_4/CuO): Modified Screen-Printed Electrode for Electrochemical Studies and Detection of Desipramine," RSC Adv., **10**(26), pp. 15171–15178.
[20] Abu-Abdeen, M., Saber, O., and Mousa, E., 2021, "Preparation and Physical Characterization of Cobalt Iron Oxide Magnetic Nanoparticles Loaded Polyvinyl Alcohol," J. Thermoplast. Compos. Mater., epub.
[21] Etheridge, M. L., Xu, Y., Rott, L., Choi, J., Glasmacher, B., and Bischof, J. C., 2014, "RF Heating of Magnetic Nanoparticles Improves the Thawing of Cryopreserved Biomaterials," Technology, **02**(03), pp. 229–242.
[22] Schildkopf, P., Ott, O. J., Frey, B., Wadepohl, M., Sauer, R., Fietkau, R., and Gaipl, U. S., 2010, "Biological Rationales and Clinical Applications of Temperature Controlled Hyperthermia—Implications for Multimodal Cancer Treatments," Curr. Med. Chem., **17**(27), pp. 3045–3057.
[23] Robinson, M. P., and Pegg, D. E., 1999, "Rapid Electromagnetic Warming of Cells and Tissues," IEEE Trans. Biomed. Eng., **46**(12), pp. 1413–1425.
[24] Stauffer, P. R., Cetas, T. C., and Jones, R. C., 1984, "Magnetic Induction Heating of Ferromagnetic Implants for Inducing Localized Hyperthermia in Deep-Seated Tumors," IEEE Trans. Biomed. Eng., **31**(2), pp. 235–251.
[25] Lucia, O., Maussion, P., Dede, E. J., and Burdio, J. M., 2014, "Induction Heating Technology and Its Applications: Past Developments, Current Technology, and Future Challenges," IEEE Trans. Ind. Electron., **61**(5), pp. 2509–2520.
[26] Silva, A. C., Oliveira, T. R., Mamani, J. B., Malheiros, S. M., Malavolta, L., Pavon, L. F., Sibov, T. T., 2011, "Application of Hyperthermia Induced by Superparamagnetic Iron Oxide Nanoparticles in Glioma Treatment," Int. J. Nanomed., **6**, pp. 591–603.
[27] Gaitas, A., and Kim, G., 2015, "Inductive Heating Kills Cells That Contribute to Plaque: A Proof-of-Concept," PeerJ, **3**, p. e929.
[28] Sasayama, T., Yoshida, T., Tanabe, K., Tsujimura, N., and Enpuku, K., 2015, "Hysteresis Loss of Fractionated Magnetic Nanoparticles for Hyperthermia Application," IEEE Trans. Magn., **51**(11), pp. 1–4.
[29] Hergt, R., Andra, W., d'Ambly, C. G., Hilger, I., Kaiser, W. A., Richter, U., and Schmidt, H. G., 1998, "Physical Limits of Hyperthermia Using Magnetite Fine Particles," IEEE Trans. Magn., **34**(5), pp. 3745–3754.
[30] Day, E. S., Morton, J. G., and West, J. L., 2009, "Nanoparticles for Thermal Cancer Therapy," ASME J. Biomech. Eng., **131**(7), p. 074001.
[31] Deatsch, A. E., and Evans, B. A., 2014, "Heating Efficiency in Magnetic Nanoparticle Hyperthermia," J. Magn. Magn. Mater., **354**, pp. 163–172.
[32] Rosenblum, D., Joshi, N., Tao, W., Karp, J. M., and Peer, D., 2018, "Progress and Challenges Towards Targeted Delivery of Cancer Therapeutics," Nat. Commun., **9**(1), p. 1410.
[33] Ulbrich, K., Holá, K., Šubr, V., Bakandritsos, A., Tuček, J., and Zbořil, R., 2016, "Targeted Drug Delivery With Polymers and Magnetic Nanoparticles: Covalent and Noncovalent Approaches, Release Control, and Clinical Studies," Chem. Rev., **116**(9), pp. 5338–5431.
[34] Du, V., Luciani, N., Richard, S., Mary, G., Gay, C., Mazuel, F., Reffay, M., Menasche, P., Agbulut, O., and Wilhelm, C., 2017, "A 3D Magnetic Tissue Stretcher for Remote Mechanical Control of Embryonic Stem Cell Differentiation," Nat. Commun., **8**(1), p. 400.
[35] Moise, S., Byrne, J. M., El Haj, A. J., and Telling, N. D., 2018, "The Potential of Magnetic Hyperthermia for Triggering the Differentiation of Cancer Cells," Nanoscale, **10**(44), pp. 20519–20525.
[36] Lee, J. H., Huh, Y. M., Jun, Y. W., Seo, J. W., Jang, J. T., Song, H. T., Kim, S., 2007, "Artificially Engineered Magnetic Nanoparticles for Ultra-Sensitive Molecular Imaging," Nat. Med., **13**(1), pp. 95–99.
[37] Wang, Z., Xue, X., Lu, H., He, Y., Lu, Z., Chen, Z., Yuan, Y., 2020, "Two-Way Magnetic Resonance Tuning and Enhanced Subtraction Imaging for Non-Invasive and Quantitative Biological Imaging," Nat. Nanotechnol., **15**(6), pp. 482–490.
[38] Galanzha, E. I., Shashkov, E. V., Kelly, T., Kim, J. W., Yang, L., and Zharov, V. P., 2009, "In Vivo Magnetic Enrichment and Multiplex Photoacoustic Detection of Circulating Tumour Cells," Nat. Nanotechnol., **4**(12), pp. 855–860.
[39] Wang, Y., Dostalek, J., and Knoll, W., 2011, "Magnetic Nanoparticle-Enhanced Biosensor Based on Grating-Coupled Surface Plasmon Resonance," Anal. Chem., **83**(16), pp. 6202–6207.
[40] Zhang, Q., Li, L., Qiao, Z., Lei, C., Fu, Y., Xie, Q., Yao, S., Li, Y., and Ying, Y., 2017, "Electrochemical Conversion of Fe_3O_4 Magnetic Nanoparticles to Electroactive Prussian Blue Analogues for Self-Sacrificial Label Biosensing of Avian Influenza Virus H5N1," Anal. Chem., **89**(22), pp. 12145–12151.
[41] Li, J. H., Santos-Otte, P., Au, B., Rentsch, J., Block, S., and Ewers, H., 2020, "Directed Manipulation of Membrane Proteins by Fluorescent Magnetic Nanoparticles," Nat. Commun., **11**(1), p. 4259.
[42] Wu, C. H., Huang, Y. Y., Chen, P., Hoshino, K., Liu, H., Frenkel, E. P., Zhang, J. X., and Sokolov, K. V., 2013, "Versatile Immunomagnetic Nanocarrier Platform for Capturing Cancer Cells," ACS Nano, **7**(10), pp. 8816–8823.
[43] Pottler, M., Fliedner, A., Bergmann, J., Bui, L. K., Muhlberger, M., Braun, C., Graw, M., 2019, "Magnetic Tissue Engineering of the Vocal Fold Using Superparamagnetic Iron Oxide Nanoparticles," Tissue Eng. Part A, **25**(21–22), pp. 1470–1477.
[44] Lee, J.-H., Jang, J.-T., Choi, J.-S., Moon, S. H., Noh, S.-H., Kim, J.-W., Kim, J.-G., Kim, I.-S., Park, K. I., and Cheon, J., 2011, "Exchange-Coupled Magnetic Nanoparticles for Efficient Heat Induction," Nat. Nanotechnol., **6**(7), pp. 418–422.
[45] Huang, H., Choi, J. K., Rao, W., Zhao, S., Agarwal, P., Zhao, G., and He, X., 2015, "Alginate Hydrogel Microencapsulation Inhibits Devitrification and Enables Large-Volume Low-CPA Cell Vitrification," Adv. Funct. Mater., **25**(44), pp. 6839–6850.
[46] Manuchehrabadi, N., Gao, Z., Zhang, J., Ring, H. L., Shao, Q., Liu, F., McDermott, M., 2017, "Improved Tissue Cryopreservation Using Inductive Heating of Magnetic Nanoparticles," Sci. Transl. Med., **9**(379), p. eaah4586.
[47] Thiesen, B., and Jordan, A., 2008, "Clinical Applications of Magnetic Nanoparticles for Hyperthermia," Int. J. Hyperthermia, **24**(6), pp. 467–474.
[48] Kennedy, J. E., 2005, "High-Intensity Focused Ultrasound in the Treatment of Solid Tumours," Nat. Rev. Cancer, **5**(4), pp. 321–327.
[49] Curra, F. P., and Crum, L. A., 2003, "Therapeutic Ultrasound: Surgery and Drug Delivery," Acoust. Sci. Technol., **24**(6), pp. 343–348.
[50] Oleson, J. R., 1984, "A Review of Magnetic Induction Methods for Hyperthermia Treatment of Cancer," IEEE Trans. Biomed. Eng., **31**(1), pp. 91–97.
[51] Rudnev, V., Loveless, D., Cook, R. L., and Black, M., 2002, *Handbook of Induction Heating*, CRC Press, Boca Raton, FL.

[52] Kriezis, E. E., Tsiboukis, T. D., Panas, S. M., and Tegopoulos, J. A., 1992, "Eddy Currents—Theory and Applications," Proc. IEEE, **80**(10), pp. 1559–1589.
[53] Liu, X., Zhang, Y., Wang, Y., Zhu, W., Li, G., Ma, X., Zhang, Y., 2020, "Comprehensive Understanding of Magnetic Hyperthermia for Improving Antitumor Therapeutic Efficacy," Theranostics, **10**(8), pp. 3793–3815.
[54] Kumar, C. S., and Mohammad, F., 2011, "Magnetic Nanomaterials for Hyperthermia-Based Therapy and Controlled Drug Delivery," Adv. Drug Delivery Rev., **63**(9), pp. 789–808.
[55] Espinosa, A., Kolosnjaj-Tabi, J., Abou-Hassan, A., Plan Sangnier, A., Curcio, A., Silva, A. K. A., Di Corato, R., 2018, "Magnetic (Hyper)Thermia or Photothermia? Progressive Comparison of Iron Oxide and Gold Nanoparticles Heating in Water, in Cells, and In Vivo," Adv. Funct. Mater., **28**(37), p. 1803660.
[56] Overgaard, K., and Overgaard, J., 1972, "Investigations on the Possibility of a Thermic Tumour Therapy. I. Short-Wave Treatment of a Transplanted Isologous Mouse Mammary Carcinoma," Eur. J. Cancer, **8**(1), pp. 65–78.
[57] Sapareto, S. A., and Dewey, W. C., 1984, "Thermal Dose Determination in Cancer Therapy," Int. J. Radiat. Oncol., Biol., Phys., **10**(6), pp. 787–800.
[58] Huang, H., Yu, K., Mohammadi, A., Karanthanasis, E., Godley, A., and Yu, J. S., 2017, "It's Getting Hot in Here: Targeting Cancer Stem-Like Cells With Hyperthermia," J. Stem Cell Transplant. Biol., **2**(2), p. 113.
[59] He, X., 2011, "Thermostability of Biological Systems: Fundamentals, Challenges, and Quantification," Open Biomed. Eng. J., **5**(1), pp. 47–73.
[60] He, X., and Bischof, J. C., 2003, "Quantification of Temperature and Injury Response in Thermal Therapy and Cryosurgery," Crit. Rev. Biomed. Eng., **31**(5–6), pp. 355–422.
[61] Diller, K. R., 2005, "Bioheat and Mass Transfer as Viewed Through a Microscope," ASME J. Biomech. Eng., **127**(1), pp. 67–84.
[62] He, X., Bhowmick, S., and Bischof, J. C., 2009, "Thermal Therapy in Urologic Systems: A Comparison of Arrhenius and Thermal Isoeffective Dose Models in Predicting Hyperthermic Injury," ASME J. Biomech. Eng., **131**(7), p. 074507.
[63] LeBrun, A., Ma, R., and Zhu, L., 2016, "Tumor Shrinkage Study in Magnetic Nanoparticle Hyperthermia Based on Designed Heating Protocols," ASME Paper No. MNHMT2016-6559.
[64] Bischof, J. C., and He, X., 2005, "Thermal Stability of Proteins," Ann. N. Y. Acad. Sci., **1066**(1), pp. 12–33.
[65] Rosenberg, B., Kemeny, G., Switzer, R. C., and Hamilton, T. C., 1971, "Quantitative Evidence for Protein Denaturation as the Cause of Thermal Death," Nature, **232**(5311), pp. 471–473.
[66] LeBrun, A., Joglekar, T., Bieberich, C., Ma, R., and Zhu, L., 2017, "Treatment Efficacy for Validating MicroCT-Based Theoretical Simulation Approach in Magnetic Nanoparticle Hyperthermia for Cancer Treatment," ASME J. Heat Transfer-Trans. ASME, **139**(5), p. 051101.
[67] Bhandari, A., and Kuchhal, P., 2019, "The Concept of High Dielectric Material for the Treatment of Liver Cancer Through Microwave Heating," J. Med. Eng. Technol., **43**(3), pp. 165–172.
[68] Kotchapradit, S., Thosdeekoraphat, T., Santalunai, S., and Thongsopa, C., 2018, "Improvement of Electric Field Focusing for Deep Hyperthermia in Breast Cancer Treatment by Using Microwave Dielectric Heating With Curved Plate Applicator," Proceedings of the 2018 Asia-Pacific Microwave Conference (APMC), Kyoto, Japan, Nov. 6–9, pp. 1474–1476.
[69] He, X., McGee, S., Coad, J. E., Schmidlin, F., Iaizzo, P. A., Swanlund, D. J., Kluge, S., Rudie, E., and Bischof, J. C., 2004, "Investigation of the Thermal and Tissue Injury Behaviour in Microwave Thermal Therapy Using a Porcine Kidney Model," Int. J. Hyperthermia, **20**(6), pp. 567–593.
[70] Xu, J., Shamul, J. G., Wang, H., Lin, J., Agarwal, P., Sun, M., Lu, X., Tkaczuk, K. H. R., and He, X., 2020, "Targeted Heating of Mitochondria Greatly Augments Nanoparticle-Mediated Cancer Chemotherapy," Adv. Healthcare Mater., **9**(14), p. e2000181.
[71] Wang, H., Liang, Y., Yin, Y., Zhang, J., Su, W., White, A. M., Bin, J., 2021, "Carbon Nano-Onion-Mediated Dual Targeting of P-Selectin and P-Glycoprotein to Overcome Cancer Drug Resistance," Nat. Commun., **12**(1), p. 312.
[72] Lovell, J. F., Jin, C. S., Huynh, E., Jin, H., Kim, C., Rubinstein, J. L., Chan, W. C., Cao, W., Wang, L. V., and Zheng, G., 2011, "Porphysome Nanovesicles Generated by Porphyrin Bilayers for Use as Multimodal Biophotonic Contrast Agents," Nat. Mater., **10**(4), pp. 324–332.
[73] Khokhlova, A., Zolotovskii, I., Stoliarov, D., Vorsina, S., Liamina, D., Pogodina, E., Fotiadi, A. A., Sokolovski, S. G., Saenko, Y., and Rafailov, E. U., 2019, "The Photobiomodulation of Vital Parameters of the Cancer Cell Culture by Low Dose of Near-IR Laser Irradiation," IEEE J. Sel. Top. Quantum Electron., **25**(1), pp. 1–10.
[74] Wang, T., Wang, D., Yu, H., Feng, B., Zhou, F., Zhang, H., Zhou, L., Jiao, S., and Li, Y., 2018, "A Cancer Vaccine-Mediated Postoperative Immunotherapy for Recurrent and Metastatic Tumors," Nat. Commun., **9**(1), p. 1532.
[75] Wang, H., Agarwal, P., Zhao, S., Yu, J., Lu, X., and He, X., 2015, "A Biomimetic Hybrid Nanoplatform for Encapsulation and Precisely Controlled Delivery of Theranostic Agents," Nat. Commun., **6**(1), p. 10081.
[76] Roizin-Towle, L., and Pirro, J. P., 1991, "The Response of Human and Rodent Cells to Hyperthermia," Int. J. Radiat. Oncol., Biol., Phys., **20**(4), pp. 751–756.
[77] Dennis, C. L., and Ivkov, R., 2013, "Physics of Heat Generation Using Magnetic Nanoparticles for Hyperthermia," Int. J. Hyperthermia, **29**(8), pp. 715–729.
[78] Banobre-Lopez, M., Teijeiro, A., and Rivas, J., 2013, "Magnetic Nanoparticle-Based Hyperthermia for Cancer Treatment," Rep. Pract. Oncol. Radiother., **18**(6), pp. 397–400.
[79] Kossatz, S., Grandke, J., Couleaud, P., Latorre, A., Aires, A., Crosbie-Staunton, K., Ludwig, R., 2015, "Efficient Treatment of Breast Cancer Xenografts With Multifunctionalized Iron Oxide Nanoparticles Combining Magnetic Hyperthermia and Anti-Cancer Drug Delivery," Breast Cancer Res., **17**(1), p. 66.
[80] Chang, D., Lim, M., Goos, J., Qiao, R., Ng, Y. Y., Mansfeld, F. M., Jackson, M., Davis, T. P., and Kavallaris, M., 2018, "Biologically Targeted Magnetic Hyperthermia: Potential and Limitations," Front. Pharmacol., **9**(831), p. 831.
[81] Obaidat, I. M., Issa, B., and Haik, Y., 2015, "Magnetic Properties of Magnetic Nanoparticles for Efficient Hyperthermia," Nanomaterials (Basel), **5**(1), pp. 63–89.
[82] Dutz, S., and Hergt, R., 2013, "Magnetic Nanoparticle Heating and Heat Transfer on a Microscale: Basic Principles, Realities and Physical Limitations of Hyperthermia for Tumour Therapy," Int. J. Hyperthermia, **29**(8), pp. 790–800.
[83] Johannsen, M., Gneveckow, U., Taymoorian, K., Thiesen, B., Waldofner, N., Scholz, R., Jung, K., Jordan, A., Wust, P., and Loening, S. A., 2007, "Morbidity and Quality of Life During Thermotherapy Using Magnetic Nanoparticles in Locally Recurrent Prostate Cancer: Results of a Prospective Phase I Trial," Int. J. Hyperthermia, **23**(3), pp. 315–323.
[84] Pham, H. N., Pham, T. H. G., Nguyen, D. T., Phan, Q. T., Le, T. T. H., Ha, P. T., Do, H. M., Hoang, T. M. N., and Nguyen, X. P., 2017, "Magnetic Inductive Heating of Organs of Mouse Models Treated by Copolymer Coated Fe_3O_4 Nanoparticles," Adv. Nat. Sci.: Nanosci. Nanotechnol., **8**(2), p. 025013.
[85] Liu, X. L., Fan, H. M., Yi, J. B., Yang, Y., Choo, E. S. G., Xue, J. M., Di Fan, D., and Ding, J., 2012, "Optimization of Surface Coating on Fe_3O_4 Nanoparticles for High Performance Magnetic Hyperthermia Agents," J. Mater. Chem., **22**(17), pp. 8235–8244.
[86] Fortin, J. P., Wilhelm, C., Servais, J., Menager, C., Bacri, J. C., and Gazeau, F., 2007, "Size-Sorted Anionic Iron Oxide Nanomagnets as Colloidal Mediators for Magnetic Hyperthermia," J. Am. Chem. Soc., **129**(9), pp. 2628–2635.
[87] Nemati, Z., Alonso, J., Martinez, L. M., Khurshid, H., Garaio, E., Garcia, J. A., Phan, M. H., and Srikanth, H., 2016, "Enhanced Magnetic Hyperthermia in Iron Oxide Nano-Octopods: Size and Anisotropy Effects," J. Phys. Chem. C, **120**(15), pp. 8370–8379.
[88] Giustini, A. J., Ivkov, R., and Hoopes, P. J., 2011, "Magnetic Nanoparticle Biodistribution Following Intratumoral Administration," Nanotechnology, **22**(34), p. 345101.
[89] Wang, L., Huang, J., Chen, H., Wu, H., Xu, Y., Li, Y., Yi, H., Wang, Y. A., Yang, L., and Mao, H., 2017, "Exerting Enhanced Permeability and Retention Effect Driven Delivery by Ultrafine Iron Oxide Nanoparticles With T1-T2 Switchable Magnetic Resonance Imaging Contrast," ACS Nano, **11**(5), pp. 4582–4592.
[90] Liu, X. L., and Fan, H. M., 2014, "Innovative Magnetic Nanoparticle Platform for Magnetic Resonance Imaging and Magnetic Fluid Hyperthermia Applications," Curr. Opin. Chem. Eng., **4**, pp. 38–46.
[91] Du, Y., Liu, X., Liang, Q., Liang, X. J., and Tian, J., 2019, "Optimization and Design of Magnetic Ferrite Nanoparticles With Uniform Tumor Distribution for Highly Sensitive MRI/MPI Performance and Improved Magnetic Hyperthermia Therapy," Nano Lett., **19**(6), pp. 3618–3626.
[92] Bonilla, A. M., and Gonzalez, P. H., 2017, "Hybrid Polymeric-Magnetic Nanoparticles in Cancer Treatments," Curr. Pharm. Des., **23**(35), pp. 5392–5402.
[93] van Landeghem, F. K. H., Maier-Hauff, K., Jordan, A., Hoffmann, K.-T., Gneveckow, U., Scholz, R., Thiesen, B., Brück, W., and von Deimling, A., 2009, "Post-Mortem Studies in Glioblastoma Patients Treated With Thermotherapy Using Magnetic Nanoparticles," Biomaterials, **30**(1), pp. 52–57.
[94] Zhang, J., Dewilde, A. H., Chinn, P., Foreman, A., Barry, S., Kanne, D., and Braunhut, S. J., 2011, "Herceptin-Directed Nanoparticles Activated by an Alternating Magnetic Field Selectively Kill HER-2 Positive Human Breast Cells In Vitro Via Hyperthermia," Int. J. Hyperthermia, **27**(7), pp. 682–697.
[95] DeNardo, S. J., DeNardo, G. L., Natarajan, A., Miers, L. A., Foreman, A. R., Gruettner, C., Adamson, G. N., and Ivkov, R., 2007, "Thermal Dosimetry Predictive of Efficacy of 111In-ChL6 Nanoparticle AMF-Induced Thermoablative Therapy for Human Breast Cancer in Mice," J. Nucl. Med., **48**(3), pp. 437–444.
[96] Thomas, R. G., Moon, M. J., Lee, H., Sasikala, A. R., Kim, C. S., Park, I. K., and Jeong, Y. Y., 2015, "Hyaluronic Acid Conjugated Superparamagnetic Iron Oxide Nanoparticle for Cancer Diagnosis and Hyperthermia Therapy," Carbohydr. Polym., **131**, pp. 439–446.
[97] Cędrowska, E., Pruszyński, M., Gawęda, W., Żuk, M., Krysiński, P., Bruchertseifer, F., Morgenstern, A., Karageorgou, M.-A., Bouziotis, P., and Bilewicz, A., 2020, "Trastuzumab Conjugated Superparamagnetic Iron Oxide Nanoparticles Labeled With (225)Ac as a Perspective Tool for Combined Alpha-Radioimmunotherapy and Magnetic Hyperthermia of HER2-Positive Breast Cancer," Molecules, **25**(5), p. 1025.
[98] Peng, H., Tang, J., Zheng, R., Guo, G., Dong, A., Wang, Y., and Yang, W., 2017, "Nuclear-Targeted Multifunctional Magnetic Nanoparticles for Photothermal Therapy," Adv. Healthcare Mater., **6**(7), p. 1601289.
[99] Giwa, S., Lewis, J. K., Alvarez, L., Langer, R., Roth, A. E., Church, G. M., Markmann, J. F., 2017, "The Promise of Organ and Tissue Preservation to Transform Medicine," Nat. Biotechnol., **35**(6), pp. 530–542.
[100] Fahy, G. M., Wowk, B., and Wu, J., 2006, "Cryopreservation of Complex Systems: The Missing Link in the Regenerative Medicine Supply Chain," Rejuvenation Res., **9**(2), pp. 279–291.
[101] Huang, H., He, X., and Yarmush, M. L., 2021, "Advanced Technologies for the Preservation of Mammalian Biospecimens," Nat. Biomed. Eng., **5**(8), pp. 793–804.

[102] Mazur, P., 1970, "Cryobiology: The Freezing of Biological Systems," Science, **168**(3934), pp. 939–949.
[103] Chiu-Lam, A., Staples, E., Pepine, C. J., and Rinaldi, C., 2021, "Perfusion, Cryopreservation, and Nanowarming of Whole Hearts Using Colloidally Stable Magnetic Cryopreservation Agent Solutions," Sci. Adv., **7**(2), p. eabe3005.
[104] Chang, T., and Zhao, G., 2021, "Ice Inhibition for Cryopreservation: Materials, Strategies, and Challenges," Adv. Sci., **8**(6), p. 2002425.
[105] Trounson, A., and Mohr, L., 1983, "Human Pregnancy Following Cryopreservation, Thawing and Transfer of an Eight-Cell Embryo," Nature, **305**(5936), pp. 707–709.
[106] Rienzi, L., Gracia, C., Maggiulli, R., LaBarbera, A. R., Kaser, D. J., Ubaldi, F. M., Vanderpoel, S., and Racowsky, C., 2016, "Oocyte, Embryo and Blastocyst Cryopreservation in ART: Systematic Review and Meta-Analysis Comparing Slow-Freezing Versus Vitrification to Produce Evidence for the Development of Global Guidance," Hum. Reprod. Update, **23**(2), pp. 139–155.
[107] Frederickson, R., 2000, "Cryopreservation by Vitrification," Nat. Biotechnol., **18**(3), p. 250.
[108] Rall, W. F., and Fahy, G. M., 1985, "Ice-Free Cryopreservation of Mouse Embryos at −196 °C by Vitrification," Nature, **313**(6003), pp. 573–575.
[109] Palasz, A. T., and Mapletoft, R. J., 1996, "Cryopreservation of Mammalian Embryos and Oocytes: Recent Advances," Biotechnol. Adv., **14**(2), pp. 127–149.
[110] He, X., Park, E. Y., Fowler, A., Yarmush, M. L., and Toner, M., 2008, "Vitrification by Ultra-Fast Cooling at a Low Concentration of Cryoprotectants in a Quartz Micro-Capillary: A Study Using Murine Embryonic Stem Cells," Cryobiology, **56**(3), pp. 223–232.
[111] Zhan, L., Guo, S.-Z., Kangas, J., Shao, Q., Shiao, M., Khosla, K., Low, W. C., McAlpine, M. C., and Bischof, J., 2021, "Conduction Cooling and Plasmonic Heating Dramatically Increase Droplet Vitrification Volumes for Cell Cryopreservation," Adv. Sci., **8**((11), p. 2004605.
[112] Finger, E. B., and Bischof, J. C., 2018, "Cryopreservation by Vitrification: A Promising Approach for Transplant Organ Banking," Curr. Opin. Organ Transplant., **23**(3), pp. 353–360.
[113] Fahy, G. M., Wowk, B., Wu, J., Phan, J., Rasch, C., Chang, A., and Zendejas, E., 2004, "Cryopreservation of Organs by Vitrification: Perspectives and Recent Advances," Cryobiology, **48**(2), pp. 157–178.
[114] Hopkins, J. B., Badeau, R., Warkentin, M., and Thorne, R. E., 2012, "Effect of Common Cryoprotectants on Critical Warming Rates and Ice Formation in Aqueous Solutions," Cryobiology, **65**(3), pp. 169–178.
[115] Akiyama, Y., Shinose, M., Watanabe, H., Yamada, S., and Kanda, Y., 2019, "Cryoprotectant-Free Cryopreservation of Mammalian Cells by Superflash Freezing," Proc. Natl. Acad. Sci. U. S. A., **116**(16), pp. 7738–7743.
[116] Peyridieu, J. F., Baudot, A., Boutron, P., Mazuer, J., Odin, J., Ray, A., Chapelier, E., Payen, E., and Descotes, J. L., 1996, "Critical Cooling and Warming Rates to Avoid Ice Crystallization in Small Pieces of Mammalian Organs Permeated With Cryoprotective Agents," Cryobiology, **33**(4), pp. 436–446.
[117] Fahy, G. M., and Wowk, B., 2015, "Principles of Cryopreservation by Vitrification," *Cryopreservation and Freeze-Drying Protocols*, W. F. Wolkers and H. Oldenhof, eds., Springer, New York, pp. 21–82.
[118] Fowler, A., and Toner, M., 2005, "Cryo-Injury and Biopreservation," Ann. N. Y. Acad. Sci., **1066**(1), pp. 119–135.
[119] Jin, B., Kusanagi, K., Ueda, M., Seki, S., Valdez, D. M., Jr., Edashige, K., and Kasai, M., 2008, "Formation of Extracellular and Intracellular Ice During Warming of Vitrified Mouse Morulae and Its Effect on Embryo Survival," Cryobiology, **56**(3), pp. 233–240.
[120] He, X., and Bischof, J. C., 2005, "Analysis of Thermal Stress in Cryosurgery of Kidneys," ASME J. Biomech. Eng., **127**(4), pp. 656–661.
[121] Solanki, P. K., Bischof, J. C., and Rabin, Y., 2017, "Thermo-Mechanical Stress Analysis of Cryopreservation in Cryobags and the Potential Benefit of Nanowarming," Cryobiology, **76**, pp. 129–139.
[122] Rabin, Y., Steif, P. S., Taylor, M. J., Julian, T. B., and Wolmark, N., 1996, "An Experimental Study of the Mechanical Response of Frozen Biological Tissues at Cryogenic Temperatures," Cryobiology, **33**(4), pp. 472–482.
[123] Etheridge, M. L., Campbell, S. A., Erdman, A. G., Haynes, C. L., Wolf, S. M., and McCullough, J., 2013, "The Big Picture on Nanomedicine: The State of Investigational and Approved Nanomedicine Products," Nanomedicine, **9**(1), pp. 1–14.
[124] Kim, B. Y., Rutka, J. T., and Chan, W. C., 2010, "Nanomedicine," N. Engl. J. Med., **363**(25), pp. 2434–2443.
[125] Wang, J., Zhao, G., Zhang, Z., Xu, X., and He, X., 2016, "Magnetic Induction Heating of Superparamagnetic Nanoparticles During Rewarming Augments the Recovery of hUCM-MSCs Cryopreserved by Vitrification," Acta Biomater., **33**, pp. 264–274.
[126] Hergt, R., Dutz, S., and Zeisberger, M., 2010, "Validity Limits of the Neel Relaxation Model of Magnetic Nanoparticles for Hyperthermia," Nanotechnology, **21**(1), p. 015706.
[127] Liu, X., Zhao, G., Chen, Z., Panhwar, F., and He, X., 2018, "Dual Suppression Effect of Magnetic Induction Heating and Microencapsulation on Ice Crystallization Enables Low-Cryoprotectant Vitrification of Stem Cell-Alginate Hydrogel Constructs," ACS Appl. Mater. Interfaces, **10**(19), pp. 16822–16835.
[128] Gao, Z., Ring, H. L., Sharma, A., Namsrai, B., Tran, N., Finger, E. B., Garwood, M., Haynes, C. L., and Bischof, J. C., 2020, "Preparation of Scalable Silica-Coated Iron Oxide Nanoparticles for Nanowarming," Adv. Sci. (Weinheim), **7**(4), p. 1901624.
[129] Pan, J., Ren, S., Sekar, P. K., Peng, J., Shu, Z., Zhao, G., Ding, W., Chen, M., and Gao, D., 2019, "Investigation of Electromagnetic Resonance Rewarming Enhanced by Magnetic Nanoparticles for Cryopreservation," Langmuir, **35**(23), pp. 7560–7570.
[130] Riedinger, A., Guardia, P., Curcio, A., Garcia, M. A., Cingolani, R., Manna, L., and Pellegrino, T., 2013, "Subnanometer Local Temperature Probing and Remotely Controlled Drug Release Based on Azo-Functionalized Iron Oxide Nanoparticles," Nano Lett., **13**(6), pp. 2399–2406.
[131] Kut, C., Zhang, Y., Hedayati, M., Zhou, H., Cornejo, C., Bordelon, D., Mihalic, J., 2012, "Preliminary Study of Injury From Heating Systemically Delivered, Nontargeted Dextran-Superparamagnetic Iron Oxide Nanoparticles in Mice," Nanomedicine (London), **7**(11), pp. 1697–1711.
[132] Mornet, S., Vasseur, S., Grasset, F., Veverka, P., Goglio, G., Demourgues, A., Portier, J., Pollert, E., and Duguet, E., 2006, "Magnetic Nanoparticle Design for Medical Applications," Prog. Solid State Chem., **34**(2–4), pp. 237–247.
[133] Hussain, S. M., Hess, K. L., Gearhart, J. M., Geiss, K. T., and Schlager, J. J., 2005, "In Vitro Toxicity of Nanoparticles in BRL 3A Rat Liver Cells," Toxicol. In Vitro, **19**(7), pp. 975–983.
[134] Naqvi, S., Samim, M., Abdin, M., Ahmed, F. J., Maitra, A., Prashant, C., and Dinda, A. K., 2010, "Concentration-Dependent Toxicity of Iron Oxide Nanoparticles Mediated by Increased Oxidative Stress," Int. J. Nanomed., **5**, pp. 983–989.
[135] Cao, Y., Zhao, G., Panhwar, F., Zhang, X., Chen, Z., Cheng, L., Zang, C., Liu, F., Zhao, Y., and He, X., 2019, "The Unusual Properties of Polytetrafluoroethylene Enable Massive-Volume Vitrification of Stem Cells With Low-Concentration Cryoprotectants," Adv. Mater. Technol., **4**(1), p. 1800289.
[136] Chen, G., 1996, "Nonlocal and Nonequilibrium Heat Conduction in the Vicinity of Nanoparticles," ASME J. Heat Transfer-Trans. ASME, **118**(3), pp. 539–545.
[137] Iakoubovskii, K., Mitsuishi, K., Nakayama, Y., and Furuya, K., 2008, "Mean Free Path of Inelastic Electron Scattering in Elemental Solids and Oxides Using Transmission Electron Microscopy: Atomic Number Dependent Oscillatory Behavior," Phys. Rev. B, **77**(10), p. 104102.
[138] Cahill, D. G., Ford, W. K., Goodson, K. E., Mahan, G. D., Majumdar, A., Maris, H. J., Merlin, R., and Phillpot, S. R., 2003, "Nanoscale Thermal Transport," J. Appl. Phys., **93**(2), pp. 793–818.
[139] Siemens, M. E., Li, Q., Yang, R., Nelson, K. A., Anderson, E. H., Murnane, M. M., and Kapteyn, H. C., 2010, "Quasi-Ballistic Thermal Transport From Nanoscale Interfaces Observed Using Ultrafast Coherent Soft X-Ray Beams," Nat. Mater., **9**(1), pp. 26–30.
[140] Périgo, E. A., Hemery, G., Sandre, O., Ortega, D., Garaio, E., Plazaola, F., and Teran, F. J., 2015, "Fundamentals and Advances in Magnetic Hyperthermia," Appl. Phys. Rev., **2**(4), p. 041302.
[141] Merabia, S., Shenogin, S., Joly, L., Keblinski, P., and Barrat, J. L., 2009, "Heat Transfer From Nanoparticles: A Corresponding State Analysis," Proc. Natl. Acad. Sci. U. S. A., **106**(36), pp. 15113–15118.
[142] Cao, Y., Hassan, M., Cheng, Y., Chen, Z., Wang, M., Zhang, X., Haider, Z., and Zhao, G., 2019, "Multifunctional Photo- and Magnetoresponsive Graphene Oxide-Fe_3O_4 Nanocomposite-Alginate Hydrogel Platform for Ice Recrystallization Inhibition," ACS Appl. Mater. Interfaces, **11**(13), pp. 12379–12388.
[143] Ali, L. M. A., Shaker, S. A., Pinol, R., Millan, A., Hanafy, M. Y., Helmy, M. H., Kamel, M. A., and Mahmoud, S. A., 2020, "Effect of Superparamagnetic Iron Oxide Nanoparticles on Glucose Homeostasis on Type 2 Diabetes Experimental Model," Life Sci., **245**, p. 117361.
[144] Dini, S., Zakeri, M., Ebrahimpour, S., Dehghanian, F., and Esmaeili, A., 2021, "Quercetinconjugated Superparamagnetic Iron Oxide Nanoparticles Modulate Glucose Metabolism-Related Genes and miR-29 Family in the Hippocampus of Diabetic Rats," Sci. Rep., **11**(1), p. 8618.
[145] Stanley, S. A., Gagner, J. E., Damanpour, S., Yoshida, M., Dordick, J. S., and Friedman, J. M., 2012, "Radio-Wave Heating of Iron Oxide Nanoparticles Can Regulate Plasma Glucose in Mice," Science, **336**(6081), pp. 604–608.
[146] Chaussy, C., Thuroff, S., Rebillard, X., and Gelet, A., 2005, "Technology Insight: High-Intensity Focused Ultrasound for Urologic Cancers," Nat. Clin. Pract. Urol., **2**(4), pp. 191–198.
[147] Chaussy, C. G., and Thuroff, S. F., 2011, "Robotic High-Intensity Focused Ultrasound for Prostate Cancer: What Have We Learned in 15 Years of Clinical Use?," Curr. Urol. Rep., **12**(3), pp. 180–187.
[148] Marques, R. E., Ferreira, N. P., Sousa, D. C., Barata, A. D., Sens, P., Marques-Neves, C., and Abegão Pinto, L., 2021, "High Intensity Focused Ultrasound for Glaucoma: 1-Year Results From a Prospective Pragmatic Study," Eye (London), **35**(2), pp. 484–489.
[149] Piper, R. J., Hughes, M. A., Moran, C. M., and Kandasamy, J., 2016, "Focused Ultrasound as a Non-Invasive Intervention for Neurological Disease: A Review," Br. J. Neurosurg., **30**(3), pp. 286–293.
[150] Jenne, J. W., Preusser, T., and Gunther, M., 2012, "High-Intensity Focused Ultrasound: Principles, Therapy Guidance, Simulations and Applications," Z. Med. Phys., **22**(4), pp. 311–322.
[151] Abu-Zidan, F. M., Hefny, A. F., and Corr, P., 2011, "Clinical Ultrasound Physics," J. Emerg., Trauma, Shock, **4**(4), pp. 501–503.
[152] Bailey, M. R., Khokhlova, V. A., Sapozhnikov, O. A., Kargl, S. G., and Crum, L. A., 2003, "Physical Mechanisms of the Therapeutic Effect of Ultrasound—(A Review)," Acoust. Phys., **49**(4), pp. 369–388.
[153] Warde, N., 2010, "Prostate Cancer: High-Intensity Focused Ultrasound Therapy: Effects on Urinary and Erectile Function and Quality of Life," Nat. Rev. Urol., **7**(10), p. 531.

[154] Haar, G. T., and Coussios, C., 2007, "High Intensity Focused Ultrasound: Physical Principles and Devices," Int. J. Hyperthermia, **23**(2), pp. 89–104.
[155] Zhou, Y. F., 2011, "High Intensity Focused Ultrasound in Clinical Tumor Ablation," World J. Clin. Oncol., **2**(1), pp. 8–27.
[156] Wu, F., Wang, Z. B., Cao, Y. D., Chen, W. Z., Bai, J., Zou, J. Z., and Zhu, H., 2003, "A Randomised Clinical Trial of High-Intensity Focused Ultrasound Ablation for the Treatment of Patients With Localised Breast Cancer," Br. J. Cancer, **89**(12), pp. 2227–2233.
[157] Illing, R. O., Kennedy, J. E., Wu, F., ter Haar, G. R., Protheroe, A. S., Friend, P. J., Gleeson, F. V., Cranston, D. W., Phillips, R. R., and Middleton, M. R., 2005, "The Safety and Feasibility of Extracorporeal High-Intensity Focused Ultrasound (HIFU) for the Treatment of Liver and Kidney Tumours in a Western Population," Br. J. Cancer, **93**(8), pp. 890–895.
[158] Hutchinson, L., 2011, "Treatment Modalities: HIFU Is Effective for Unresectable HCC," Nat. Rev. Clin. Oncol., **8**(7), p. 385.
[159] Thuroff, S., Chaussy, C., Vallancien, G., Wieland, W., Kiel, H. J., Le Duc, A., Desgrandchamps, F., De La Rosette, J. J., and Gelet, A., 2003, "High-Intensity Focused Ultrasound and Localized Prostate Cancer: Efficacy Results From the European Multicentric Study," J. Endourol., **17**(8), pp. 673–677.
[160] Wu, F., Wang, Z. B., Chen, W. Z., Zou, J. Z., Bai, J., Zhu, H., Li, K. Q., 2004, "Extracorporeal Focused Ultrasound Surgery for Treatment of Human Solid Carcinomas: Early Chinese Clinical Experience," Ultrasound Med. Biol., **30**(2), pp. 245–260.
[161] Sadeghi-Goughari, M., Jeon, S., and Kwon, H. J., 2020, "Analytical and Numerical Model of High Intensity Focused Ultrasound Enhanced With Nanoparticles," IEEE Trans. Biomed. Eng., **67**(11), pp. 3083–3093.
[162] Sibille, A., Prat, F., Chapelon, J. Y., Abou el Fadil, F., Henry, L., Theillere, Y., Ponchon, T., and Cathignol, D., 1993, "Extracorporeal Ablation of Liver Tissue by High-Intensity Focused Ultrasound," Oncology, **50**(5), pp. 375–379.
[163] Dubinsky, T. J., Cuevas, C., Dighe, M. K., Kolokythas, O., and Hwang, J. H., 2008, "High-Intensity Focused Ultrasound: Current Potential and Oncologic Applications," AJR Am. J. Roentgenol., **190**(1), pp. 191–199.
[164] Devarakonda, S. B., Myers, M. R., Giridhar, D., Dibaji, S. A., and Banerjee, R. K., 2017, "Enhanced Thermal Effect Using Magnetic Nano-Particles During High-Intensity Focused Ultrasound," PLoS One, **12**(4), p. e0175093.
[165] Gianfelice, D., Khiat, A., Boulanger, Y., Amara, M., and Belblidia, A., 2003, "Feasibility of Magnetic Resonance Imaging-Guided Focused Ultrasound Surgery as an Adjunct to Tamoxifen Therapy in High-Risk Surgical Patients With Breast Carcinoma," J. Vasc. Interv. Radiol., **14**(10), pp. 1275–1282.
[166] Furusawa, H., Namba, K., Thomsen, S., Akiyama, F., Bendet, A., Tanaka, C., Yasuda, Y., and Nakahara, H., 2006, "Magnetic Resonance-Guided Focused Ultrasound Surgery of Breast Cancer: Reliability and Effectiveness," J. Am. Coll. Surg., **203**(1), pp. 54–63.
[167] Clark, A., Bonilla, S., Suo, D., Shapira, Y., and Averkiou, M., 2021, "Microbubble-Enhanced Heating: Exploring the Effect of Microbubble Concentration and Pressure Amplitude on High-Intensity Focused Ultrasound Treatments," Ultrasound Med. Biol., **47**(8), pp. 2296–2309.
[168] Kaczmarek, K., Hornowski, T., Kubovcikova, M., Timko, M., Koralewski, M., and Jozefczak, A., 2018, "Heating Induced by Therapeutic Ultrasound in the Presence of Magnetic Nanoparticles," ACS Appl. Mater. Interfaces, **10**(14), pp. 11554–11564.
[169] Ho, V. H., Smith, M. J., and Slater, N. K., 2011, "Effect of Magnetite Nanoparticle Agglomerates on the Destruction of Tumor Spheroids Using High Intensity Focused Ultrasound," Ultrasound Med. Biol., **37**(1), pp. 169–175.
[170] Ahmad Reza Dibaji, S., Al-Rjoub, M. F., Myers, M. R., and Banerjee, R. K., 2013, "Enhanced Heat Transfer and Thermal Dose Using Magnetic Nanoparticles During HIFU Thermal Ablation—An In-Vitro Study," ASME J. Nanotechnol. Eng. Med., **4**(4), p. 040902.
[171] Józefczak, A., Kaczmarek, K., Hornowski, T., Kubovčíková, M., Rozynek, Z., Timko, M., and Skumiel, A., 2016, "Magnetic Nanoparticles for Enhancing the Effectiveness of Ultrasonic Hyperthermia," Appl. Phys. Lett., **108**(26), p. 263701.
[172] Tang, H., Guo, Y., Peng, L., Fang, H., Wang, Z., Zheng, Y., Ran, H., and Chen, Y., 2018, "In Vivo Targeted, Responsive, and Synergistic Cancer Nanotheranostics by Magnetic Resonance Imaging-Guided Synergistic High-Intensity Focused Ultrasound Ablation and Chemotherapy," ACS Appl. Mater. Interfaces, **10**(18), pp. 15428–15441.
[173] Sun, Y., Zheng, Y., Ran, H., Zhou, Y., Shen, H., Chen, Y., Chen, H., 2012, "Superparamagnetic PLGA-Iron Oxide Microcapsules for Dual-Modality US/MR Imaging and High Intensity Focused U.S. Breast Cancer Ablation," Biomaterials, **33**(24), pp. 5854–5864.
[174] Zhou, D., Sun, Y., Zheng, Y. Y., Ran, H. T., Li, P., Wang, Z. B., and Wang, Z. G., 2015, "Superparamagnetic PLGA-Iron Oxide Microspheres as Contrast Agents for Dual-Imaging and the Enhancement of the Effects of High-Intensity Focused Ultrasound Ablation on Liver Tissue," RSC Adv., **5**(45), pp. 35693–35703.
[175] Dutz, S., Kettering, M., Hilger, I., Müller, R., and Zeisberger, M., 2011, "Magnetic Multicore Nanoparticles for Hyperthermia—Influence of Particle Immobilization in Tumour Tissue on Magnetic Properties," Nanotechnology, **22**(26), p. 265102.
[176] Lartigue, L., Innocenti, C., Kalaivani, T., Awwad, A., Sanchez Duque, M. D. M., Guari, Y., Larionova, J., 2011, "Water-Dispersible Sugar-Coated Iron Oxide Nanoparticles. An Evaluation of Their Relaxometric and Magnetic Hyperthermia Properties," J. Am. Chem. Soc., **133**(27), pp. 10459–10472.
[177] Moroz, P., Jones, S. K., and Gray, B. N., 2002, "Tumor Response to Arterial Embolization Hyperthermia and Direct Injection Hyperthermia in a Rabbit Liver Tumor Model," J. Surg. Oncol., **80**(3), pp. 149–156.
[178] Espinosa, A., Bugnet, M., Radtke, G., Neveu, S., Botton, G. A., Wilhelm, C., and Abou-Hassan, A., 2015, "Can Magneto-Plasmonic Nanohybrids Efficiently Combine Photothermia With Magnetic Hyperthermia?," Nanoscale, **7**(45), pp. 18872–18877.
[179] Yoo, D., Jeong, H., Noh, S.-H., Lee, J.-H., and Cheon, J., 2013, "Magnetically Triggered Dual Functional Nanoparticles for Resistance-Free Apoptotic Hyperthermia," Angew. Chem. Int. Ed., **52**(49), pp. 13047–13051.
[180] Gilchrist, R. K., Medal, R., Shorey, W. D., Hanselman, R. C., Parrott, J. C., and Taylor, C. B., 1957, "Selective Inductive Heating of Lymph Nodes," Ann. Surg., **146**(4), pp. 596–606.
[181] Iglesias, G. R., Jabalera, Y., Peigneux, A., Checa Fernández, B. L., Delgado, A. V., and Jimenez-Lopez, C., 2019, "Enhancement of Magnetic Hyperthermia by Mixing Synthetic Inorganic and Biomimetic Magnetic Nanoparticles," Pharmaceutics, **11**(6), p. 273.
[182] Alphandéry, E., Faure, S., Seksek, O., Guyot, F., and Chebbi, I., 2011, "Chains of Magnetosomes Extracted From AMB-1 Magnetotactic Bacteria for Application in Alternative Magnetic Field Cancer Therapy," ACS Nano, **5**(8), pp. 6279–6296.
[183] Gao, W., Zheng, Y., Wang, R., Chen, H., Cai, X., Lu, G., Chu, L., 2016, "A Smart, Phase Transitional and Injectable DOX/PLGA-Fe Implant for Magnetic-Hyperthermia-Induced Synergistic Tumor Eradication," Acta Biomater., **29**, pp. 298–306.
[184] Shetake, N. G., Kumar, A., Gaikwad, S., Ray, P., Desai, S., Ningthoujam, R. S., Vatsa, R. K., and Pandey, B. N., 2015, "Magnetic Nanoparticle-Mediated Hyperthermia Therapy Induces Tumour Growth Inhibition by Apoptosis and Hsp90/AKT Modulation," Int. J. Hyperthermia, **31**(8), pp. 909–919.
[185] Xie, J., Zhang, Y., Yan, C., Song, L., Wen, S., Zang, F., Chen, G., Ding, Q., Yan, C., and Gu, N., 2014, "High-Performance PEGylated Mn–Zn Ferrite Nanocrystals as a Passive-Targeted Agent for Magnetically Induced Cancer Theranostics," Biomaterials, **35**(33), pp. 9126–9136.
[186] Espinosa, A., Di Corato, R., Kolosnjaj-Tabi, J., Flaud, P., Pellegrino, T., and Wilhelm, C., 2016, "Duality of Iron Oxide Nanoparticles in Cancer Therapy: Amplification of Heating Efficiency by Magnetic Hyperthermia and Photothermal Bimodal Treatment," ACS Nano, **10**(2), pp. 2436–2446.
[187] Balasubramanian, S., Girija, A. R., Nagaoka, Y., Iwai, S., Suzuki, M., Kizhikilot, V., Yoshida, Y., Maekawa, T., and Nair, S. D., 2014, "Curcumin and 5-Fluorouracil-Loaded, Folate- and Transferrin-Decorated Polymeric Magnetic Nanoformulation: A Synergistic Cancer Therapeutic Approach, Accelerated by Magnetic Hyperthermia," Int. J. Nanomed., **9**, pp. 437–459.
[188] Tong, S., Quinto, C. A., Zhang, L., Mohindra, P., and Bao, G., 2017, "Size-Dependent Heating of Magnetic Iron Oxide Nanoparticles," ACS Nano, **11**(7), pp. 6808–6816.
[189] Ehrlich, L. E., Gao, Z., Bischof, J. C., and Rabin, Y., 2020, "Thermal Conductivity of Cryoprotective Agents Loaded With Nanoparticles, With Application to Recovery of Preserved Tissues and Organs From Cryogenic Storage," PLoS One, **15**(9), p. e0238941.
[190] Sharma, A., Rao, J. S., Han, Z., Gangwar, L., Namsrai, B., Gao, Z., Ring, H. L., 2021, "Vitrification and Nanowarming of Kidneys," Adv. Sci., **8**(19), p. 2101691.
[191] Ovejero, J. G., Armenia, I., Serantes, D., Veintemillas-Verdaguer, S., Zeballos, N., López-Gallego, F., Grüttner, C., de la Fuente, J. M., Puerto Morales, M. D., and Grazu, V., 2021, "Selective Magnetic Nanoheating: Combining Iron Oxide Nanoparticles for Multi-Hot-Spot Induction and Sequential Regulation," Nano Lett., **21**(17), pp. 7213–7220.
[192] Engelmann, U. M., Roeth, A. A., Eberbeck, D., Buhl, E. M., Neumann, U. P., Schmitz-Rode, T., and Slabu, I., 2018, "Combining Bulk Temperature and Nanoheating Enables Advanced Magnetic Fluid Hyperthermia Efficacy on Pancreatic Tumor Cells," Sci. Rep., **8**(1), p. 13210.
[193] Wust, P., Hildebrandt, B., Sreenivasa, G., Rau, B., Gellermann, J., Riess, H., Felix, R., and Schlag, P. M., 2002, "Hyperthermia in Combined Treatment of Cancer," Lancet Oncol., **3**(8), pp. 487–497.
[194] Hildebrandt, B., Wust, P., Ahlers, O., Dieing, A., Sreenivasa, G., Kerner, T., Felix, R., and Riess, H., 2002, "The Cellular and Molecular Basis of Hyperthermia," Crit. Rev. Oncol. Hematol., **43**(1), pp. 33–56.
[195] Chu, M., Shao, Y., Peng, J., Dai, X., Li, H., Wu, Q., and Shi, D., 2013, "Near-Infrared Laser Light Mediated Cancer Therapy by Photothermal Effect of Fe_3O_4 Magnetic Nanoparticles," Biomaterials, **34**(16), pp. 4078–4088.
[196] Golan, R., Bernstein, A., Sedrakyan, A., Daskivich, T. J., Du, D. T., Ehdaie, B., Fisher, B., 2018, "Development of a Nationally Representative Coordinated Registry Network for Prostate Ablation Technologies," J. Urol., **199**(6), pp. 1488–1493.
[197] Khokhlova, V. A., Fowlkes, J. B., Roberts, W. W., Schade, G. R., Xu, Z., Khokhlova, T. D., Hall, T. L., Maxwell, A. D., Wang, Y. N., and Cain, C. A., 2015, "Histotripsy Methods in Mechanical Disintegration of Tissue: Towards Clinical Applications," Int. J. Hyperthermia, **31**(2), pp. 145–162.
[198] Meng, Y., Hynynen, K., and Lipsman, N., 2021, "Applications of Focused Ultrasound in the Brain: From Thermoablation to Drug Delivery," Nat. Rev. Neurol., **17**(1), pp. 7–22.
[199] Lang, B. H., Woo, Y. C., and Chiu, K. W., 2017, "Single-Session High-Intensity Focused Ultrasound Treatment in Large-Sized Benign Thyroid Nodules," Thyroid, **27**(5), pp. 714–721.
[200] Lammers, T., Kiessling, F., Ashford, M., Hennink, W., Crommelin, D., and Storm, G., 2016, "Cancer Nanomedicine: Is Targeting Our Target?," Nat. Rev. Mater., **1**(9), p. 16069.
[201] Mu, Q., Jiang, G., Chen, L., Zhou, H., Fourches, D., Tropsha, A., and Yan, B., 2014, "Chemical Basis of Interactions Between Engineered Nanoparticles and Biological Systems," Chem. Rev., **114**(15), pp. 7740–7781.

[202] Yildirim, A., Blum, N. T., and Goodwin, A. P., 2019, "Colloids, Nanoparticles, and Materials for Imaging, Delivery, Ablation, and Theranostics by Focused Ultrasound (FUS)," Theranostics, **9**(9), pp. 2572–2594.
[203] Attaluri, A., Ma, R., and Zhu, L., 2010, "Using MicroCT Imaging Technique to Quantify Heat Generation Distribution Induced by Magnetic Nanoparticles for Cancer Treatments," ASME J. Heat Transfer-Trans. ASME, **133**(1), p. 011003.
[204] Gu, Q., Joglekar, T., Bieberich, C., Ma, R., and Zhu, L., 2019, "Nanoparticle Redistribution in PC3 Tumors Induced by Local Heating in Magnetic Nanoparticle Hyperthermia: In Vivo Experimental Study," ASME J. Heat Transfer-Trans. ASME, **141**(3), p. 032402.
[205] Khosravi, A., and Malekan, M., 2019, "Effect of the Magnetic Field on the Heat Transfer Coefficient of a Fe_3O_4-Water Ferrofluid Using Artificial Intelligence and CFD Simulation," Eur. Phys. J. Plus, **134**(3), p. 88.
[206] Hamet, P., and Tremblay, J., 2017, "Artificial Intelligence in Medicine," Metabolism, **69S**, pp. S36–S40.
[207] Adir, O., Poley, M., Chen, G., Froim, S., Krinsky, N., Shklover, J., Shainsky-Roitman, J., Lammers, T., and Schroeder, A., 2020, "Integrating Artificial Intelligence and Nanotechnology for Precision Cancer Medicine," Adv. Mater., **32**(13), p. e1901989.
[208] Wang, Y. X., 2015, "Current Status of Superparamagnetic Iron Oxide Contrast Agents for Liver Magnetic Resonance Imaging," World J. Gastroenterol., **21**(47), pp. 13400–13402.
[209] Bulte, J. W., 2009, "In Vivo MRI Cell Tracking: Clinical Studies," AJR Am. J. Roentgenol., **193**(2), pp. 314–325.
[210] Luo, S., Ma, C., Zhu, M. Q., Ju, W. N., Yang, Y., and Wang, X., 2020, "Application of Iron Oxide Nanoparticles in the Diagnosis and Treatment of Neurodegenerative Diseases With Emphasis on Alzheimer's Disease," Front. Cell. Neurosci., **14**, p. 21.
[211] Chung, T. H., Hsu, S. C., Wu, S. H., Hsiao, J. K., Lin, C. P., Yao, M., and Huang, D. M., 2018, "Dextran-Coated Iron Oxide Nanoparticle-Improved Therapeutic Effects of Human Mesenchymal Stem Cells in a Mouse Model of Parkinson's Disease," Nanoscale, **10**(6), pp. 2998–3007.